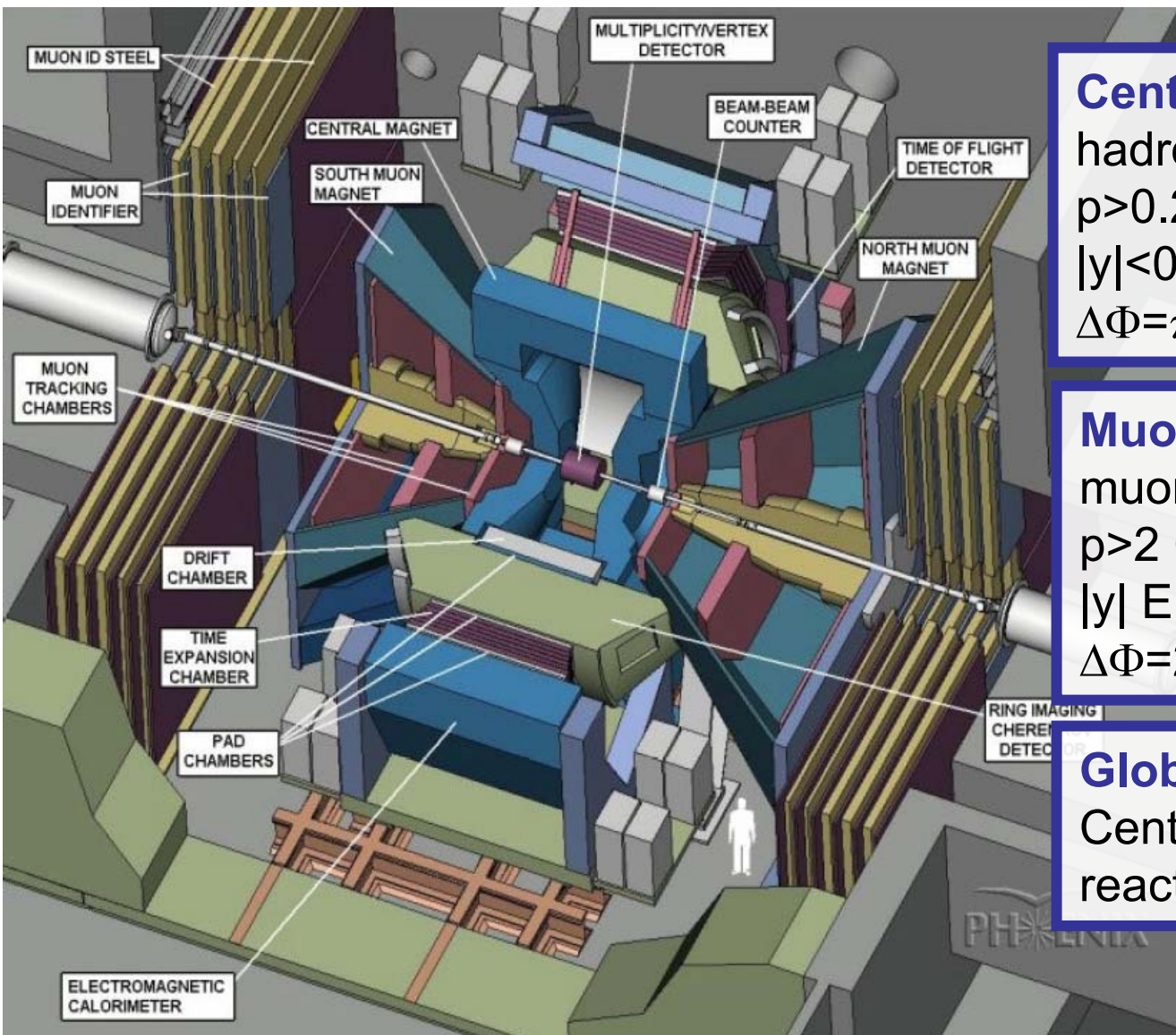


# An overview of results from the PHENIX experiment at RHIC

Hugo Pereira Da Costa, CEA Saclay, PHENIX collaboration  
Strangeness in Quark Matter, June 25 2007

# Introduction

# The PHENIX detector



## Central arm

hadrons; photons; electrons

$p > 0.2 \text{ GeV}/c$

$|y| < 0.35$

$\Delta\Phi = \pi$

## Muon arms

muons; stopped hadrons

$p > 2 \text{ GeV}/c$

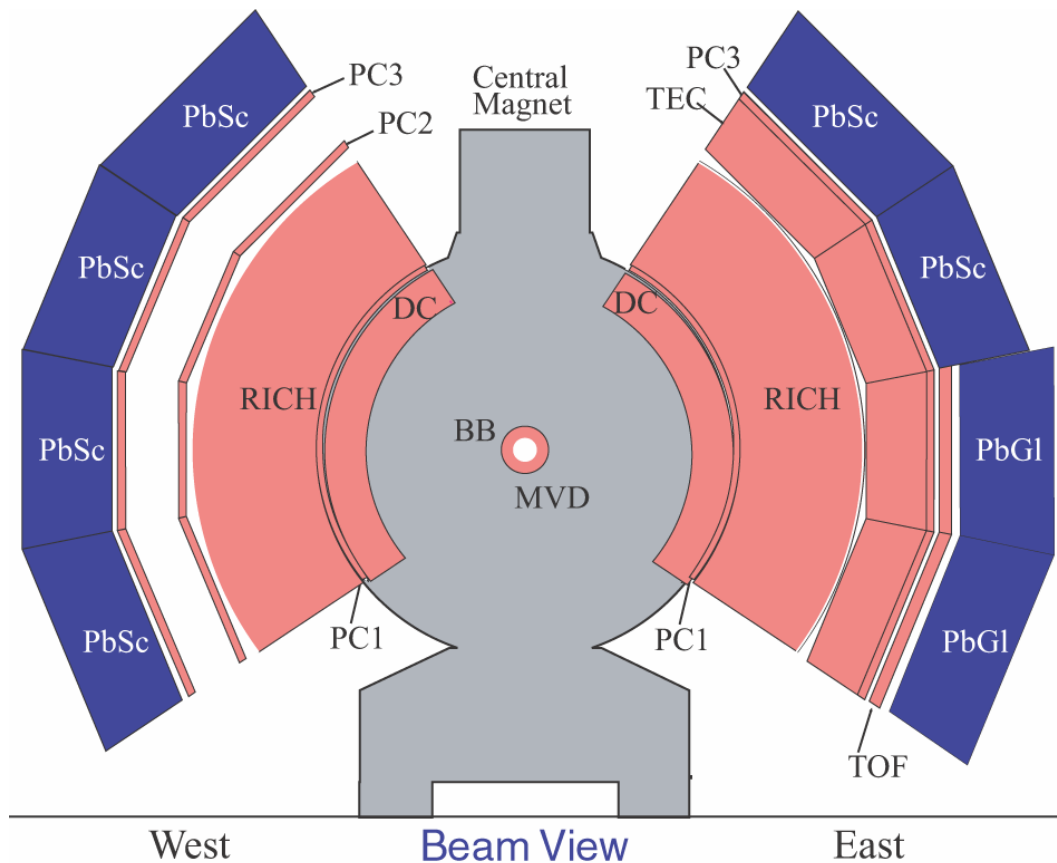
$|y| \in [1.2, 2.4]$

$\Delta\Phi = 2\pi$

## Global detectors

Centrality, vertex position,  
reaction plane

# The PHENIX detector – central arms



## Tracking:

Drift Chambers,  
Pad Chambers,  
Time Expansion Chamber

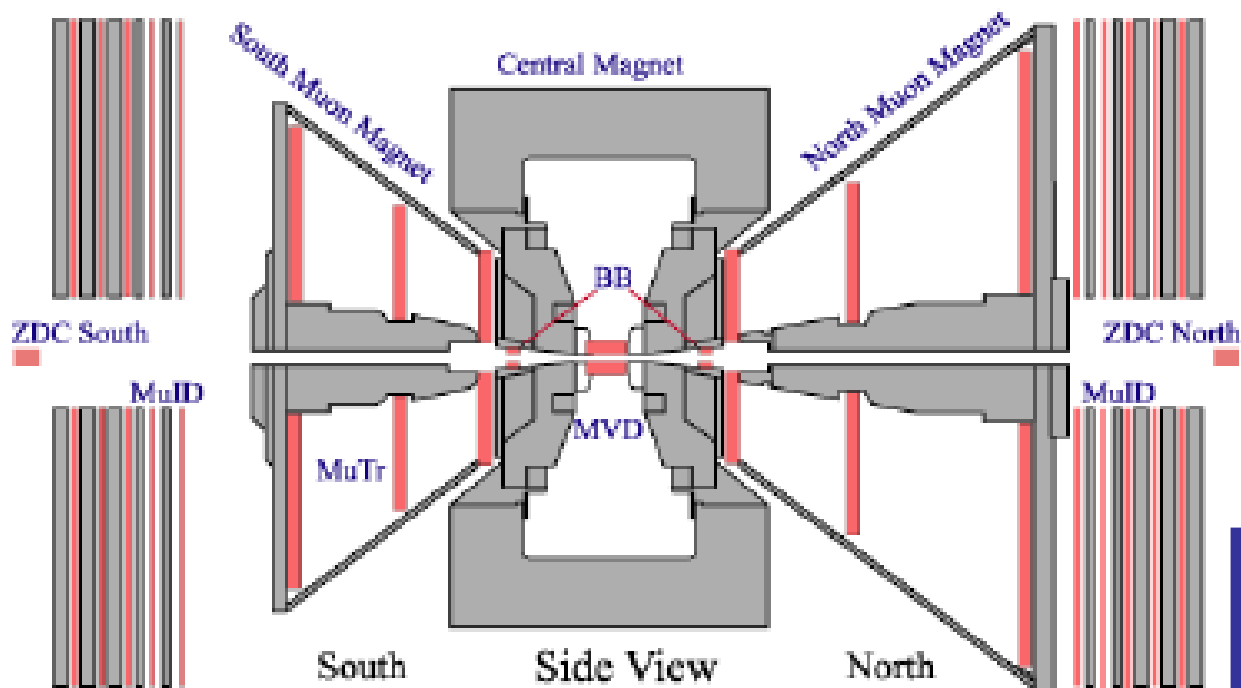
## Calorimetry:

PbGl and PbSc EMCal  
also used for triggering

## Particle identification:

RICH  
Time Of Flight

# The PHENIX detector – muon arms



## Tracking:

3 muon tracker stations of cathode strip chambers with radial magnetic field

## Muon identification:

5 detection planes (X and Y) and absorber, also used for triggering

# PHENIX capabilities

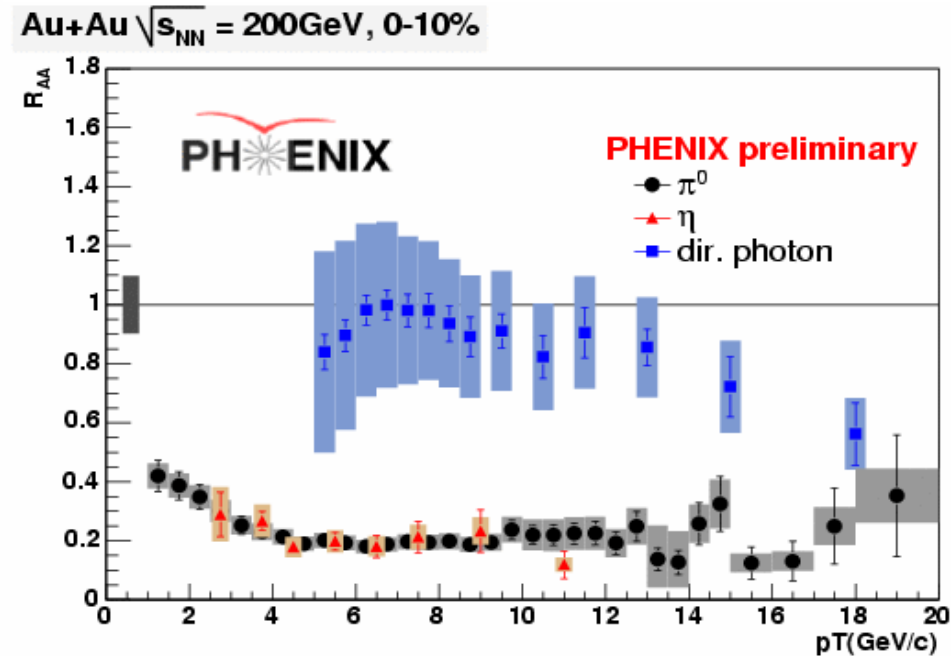
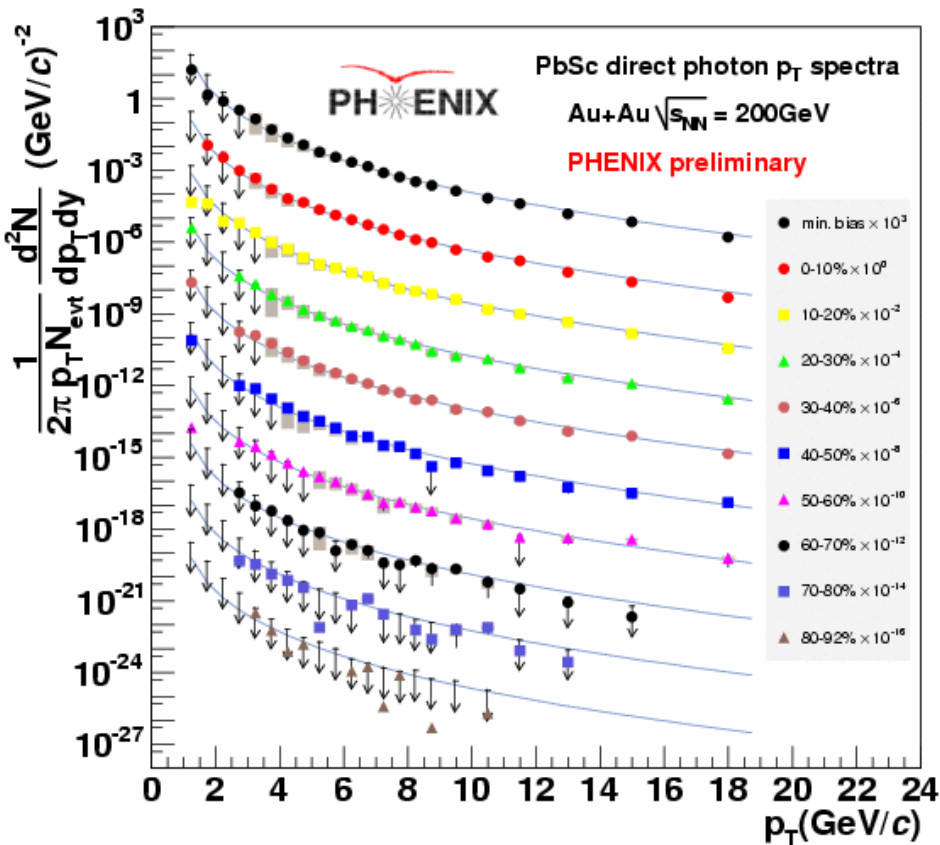
- photons  $\rightarrow$  direct photons,  $\pi^0/\eta$  over a large  $p_T$  range (0-20 GeV/c)
- charged hadrons ( $\pi^{+/-}$ ,  $K^{+/-}$ , etc.)
- light meson resonances ( $\phi$ ,  $\omega$ ,  $\eta$ ) via both electromagnetic and hadronic decays
- single leptons (electrons/muons)  $\rightarrow$  heavy flavor
- di-leptons  $\rightarrow$  heavy flavor,  $J/\Psi$  (in 2 rapidity domains)

# Outline

- energy loss (direct photons and light quarks)
- elliptic flow and thermalization
- jet correlations
- di-lepton continuum and heavy quarkonia

# Energy loss

# direct photons, $\pi^0$ and $\eta$

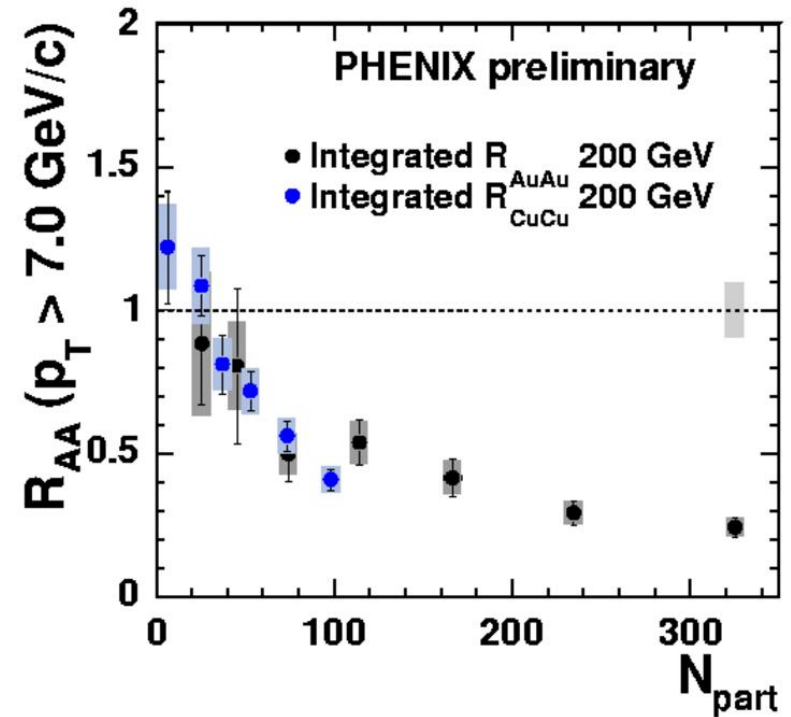
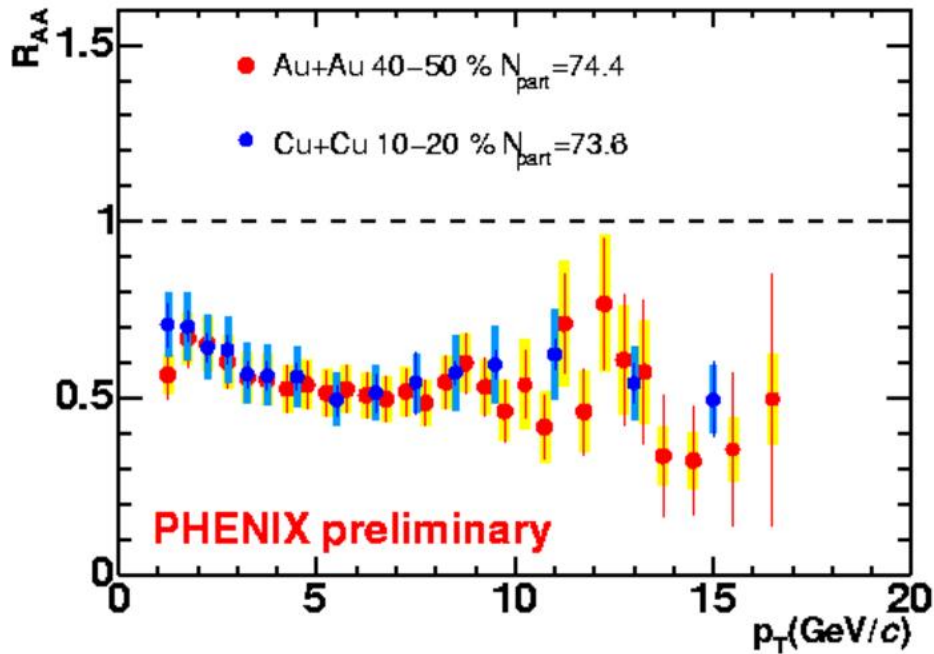


Direct photons and  $\pi^0$   $R_{AA}$  measurement extended to very high  $p_T$

New methods at low  $p_T$  (1-4 GeV/c) for photons (not shown here)

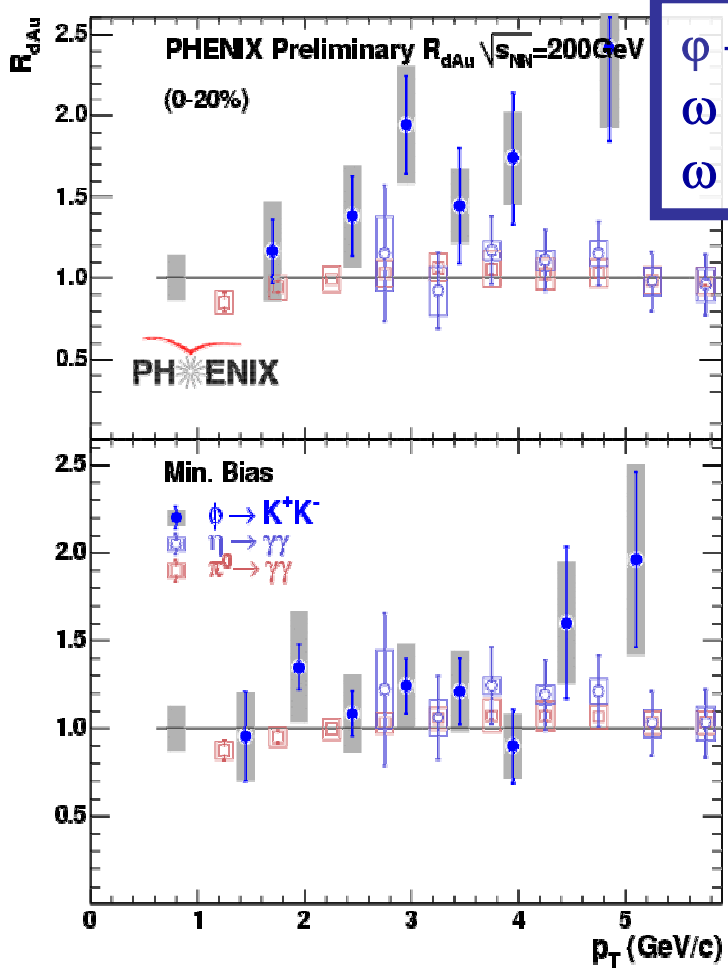
No direct photon suppression until 14 GeV  
 $\pi^0$  suppression stays nearly constant up to 20 GeV/c

# System size dependence of $\pi^0 R_{AA}$

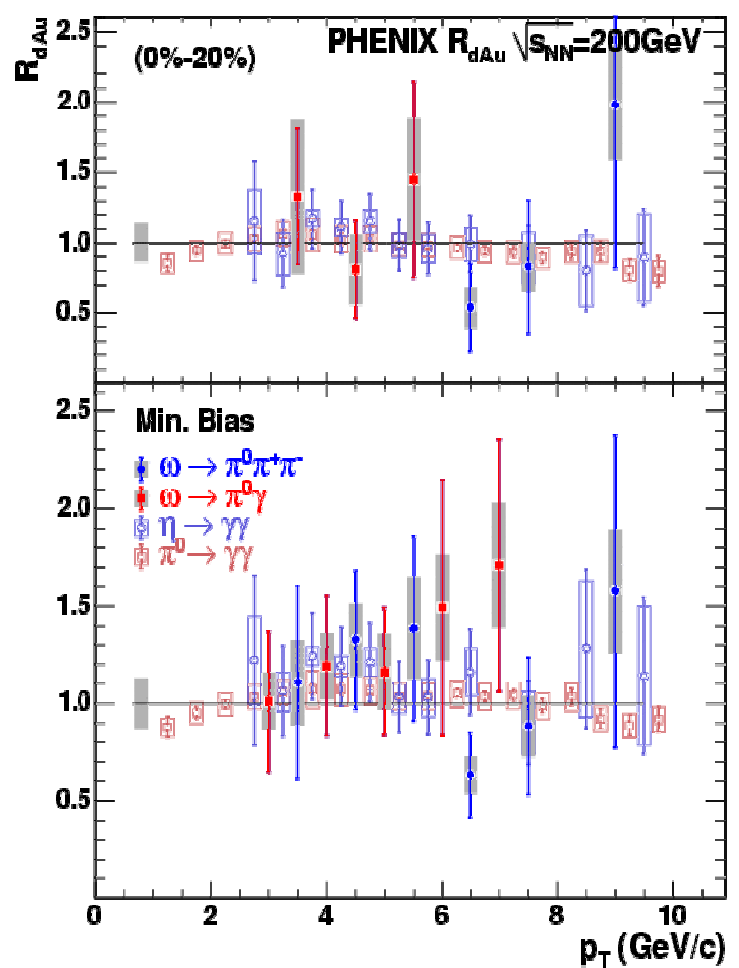


$R_{AA}$  is the same in Cu+Cu and Au+Au at equal  $N_{part}$

# Light mesons $R_{dAu}$



$R_{dAu}$  for  $\Phi$ ,  $\eta$  and  $\pi^0$  vs  $p_T$  @200 GeV in 0-20% and minimum bias

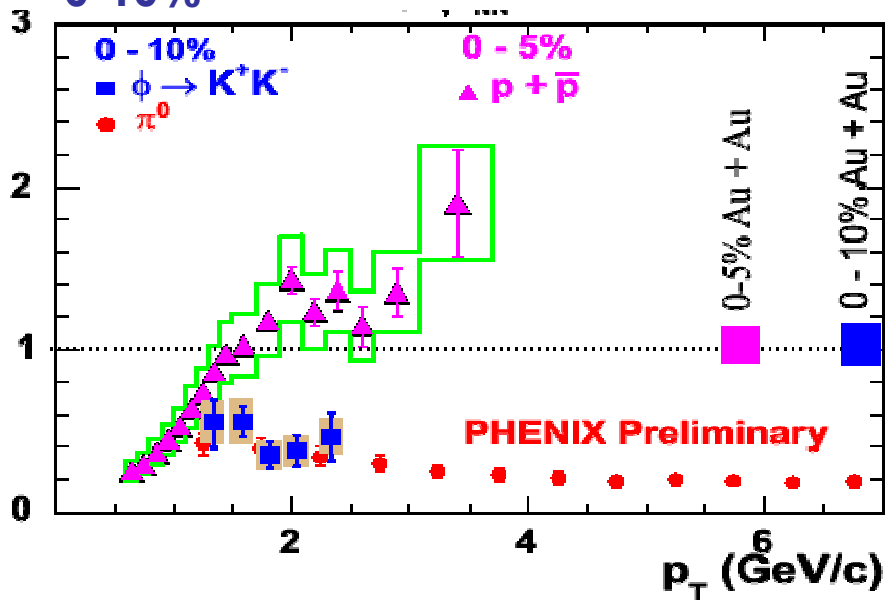


$R_{dAu}$  for  $\omega$ ,  $\eta$  and  $\pi^0$  vs  $p_T$  @200 GeV in 0-20% and minimum bias

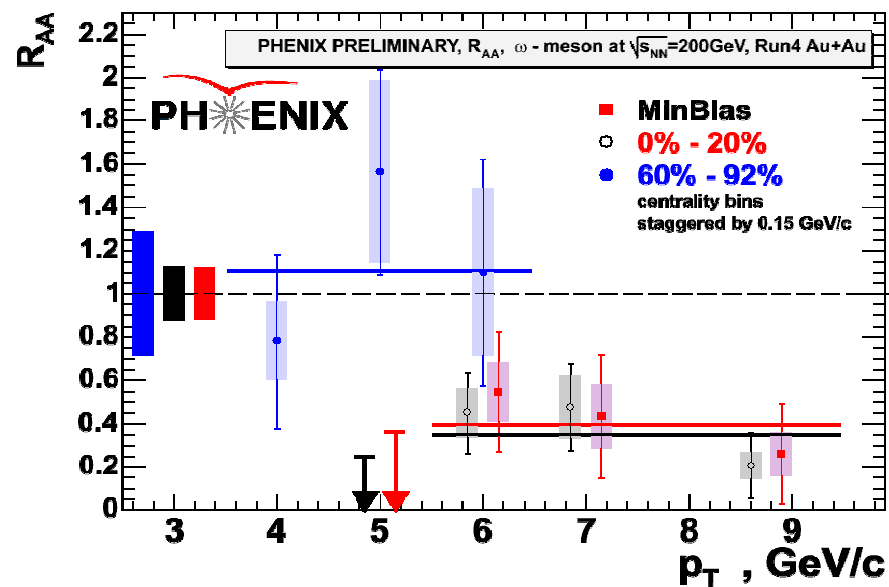
All  $R_{AA}$  are compatible with 1.  
 Large error bars prevent to quantify any cold nuclear matter effect

# light mesons $R_{AA}$

$\phi$ ,  $\rho$  and  $\pi$  in Au+Au@200 GeV  
0-10%



$\omega$  in Au+Au@200 GeV  
60-92% and 0-20%

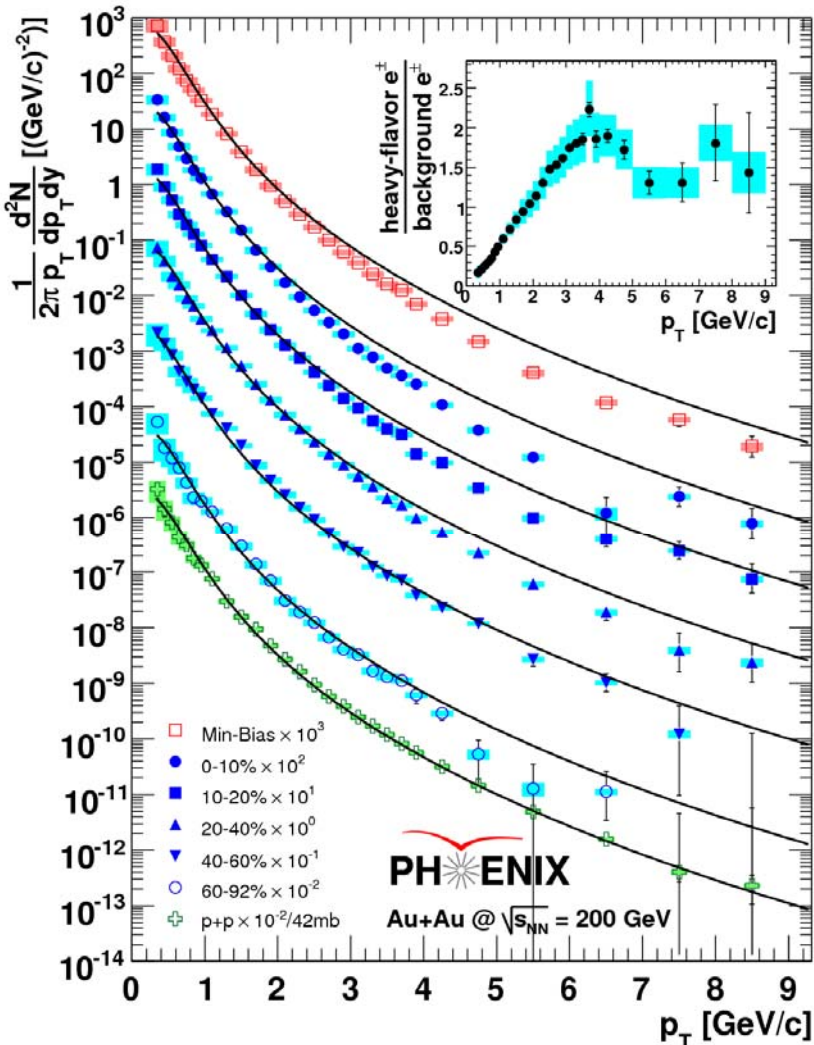


A high  $p_T$  suppression is observed for  $\phi$  and  $\omega$ ,  
similar to that observed for  $\pi$  and  $\eta$

Talk: V. Riabov, Thursday June 27

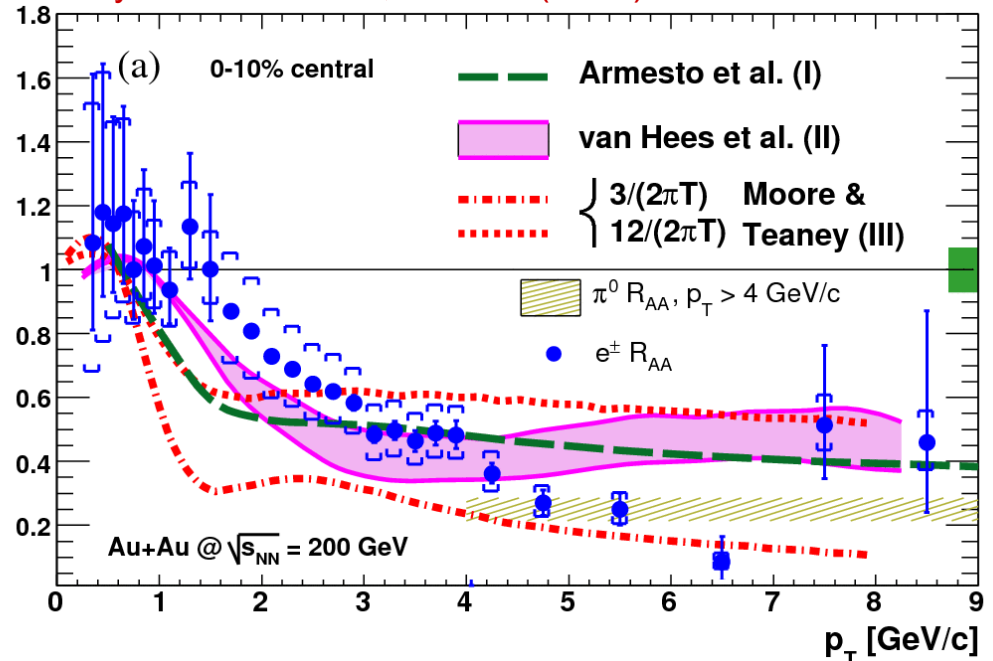
# Heavy quarks

## Non-photonic single electron vs centrality in Au+Au@200 GeV/c



## Non-photonic electron $R_{AA}$ vs $p_T$ in Au+Au@200 GeV, 0-10% central

Phys. Rev. Lett. 98, 172301 (2007)

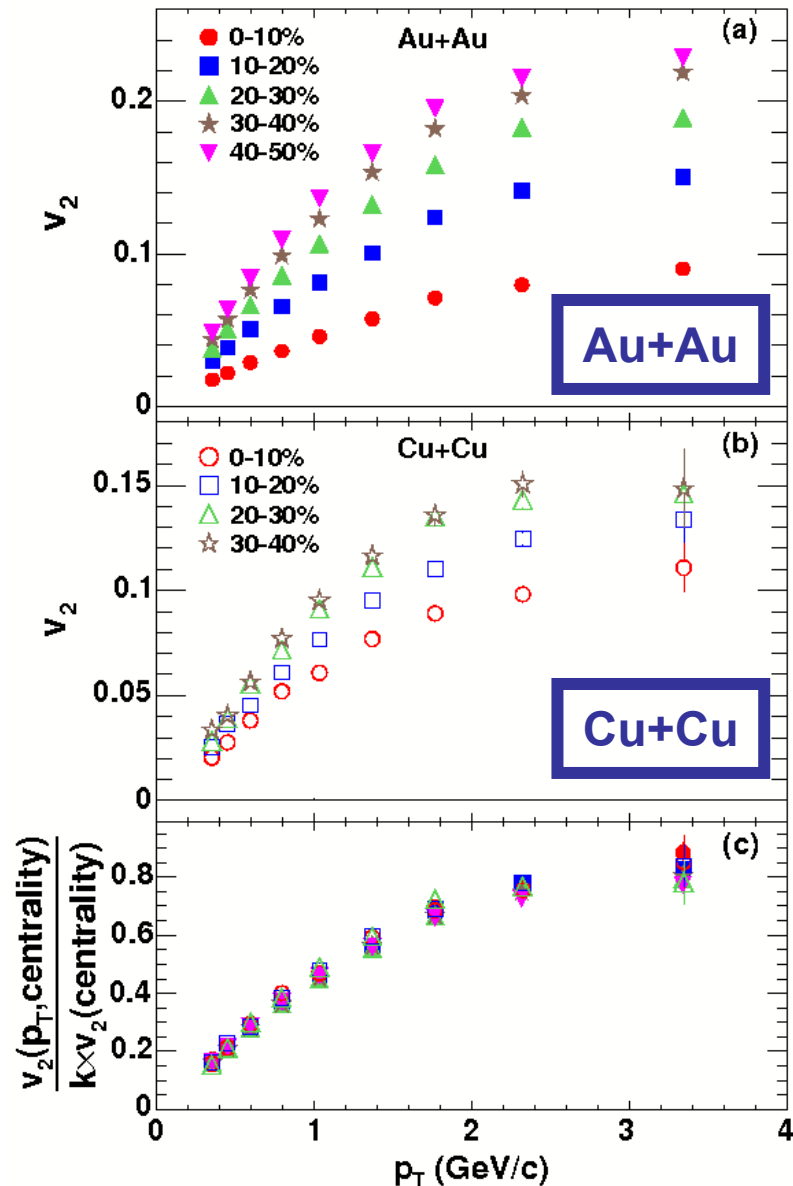


Sizeable suppression is measured.  
Slightly smaller than for pions

# Elliptic flow and thermalization

# $v_2$ vs $p_T$ , centrality and collision system

Phys. Rev Lett. 98, 162301 (2007)



The elliptic flow,  $v_2$  characterizes the azimuthal anisotropy of the medium collective motion.

$v_2$  increases from central to peripheral collisions. This is expected because the eccentricity of the overlapping area increases.

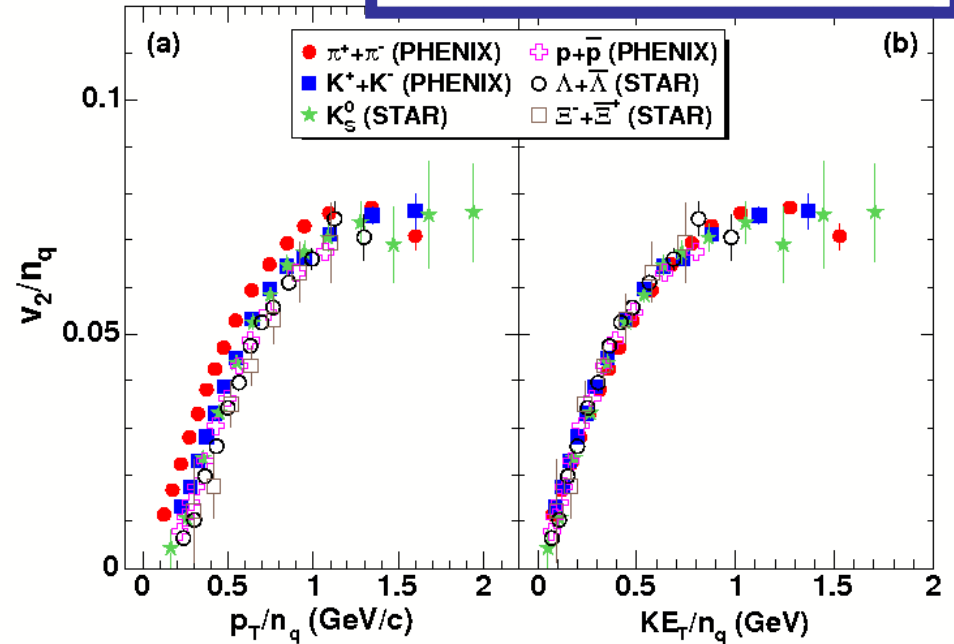
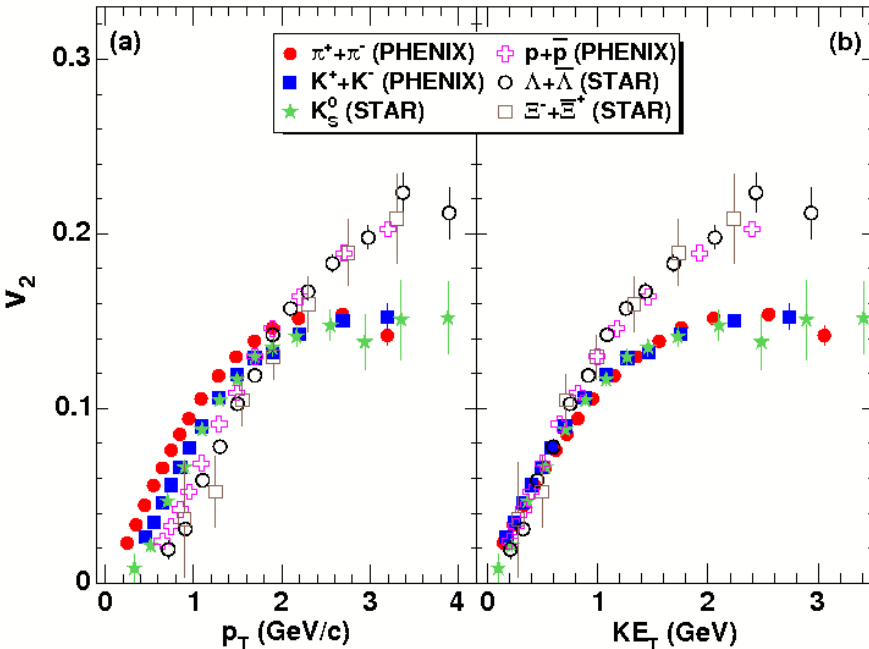
Hydrodynamic models predict that  $\int v_2$  is proportional to the eccentricity.

Differential  $v_2$  normalized to its integral is universal, meaning that the measured  $v_2$  is controlled by the geometry of the overlapping region only.

# $v_2$ vs $p_T$ , $KE_T$ and $n_q$

Phys. Rev Lett. 98, 162301 (2007)

Au+Au@200GeV min. bias



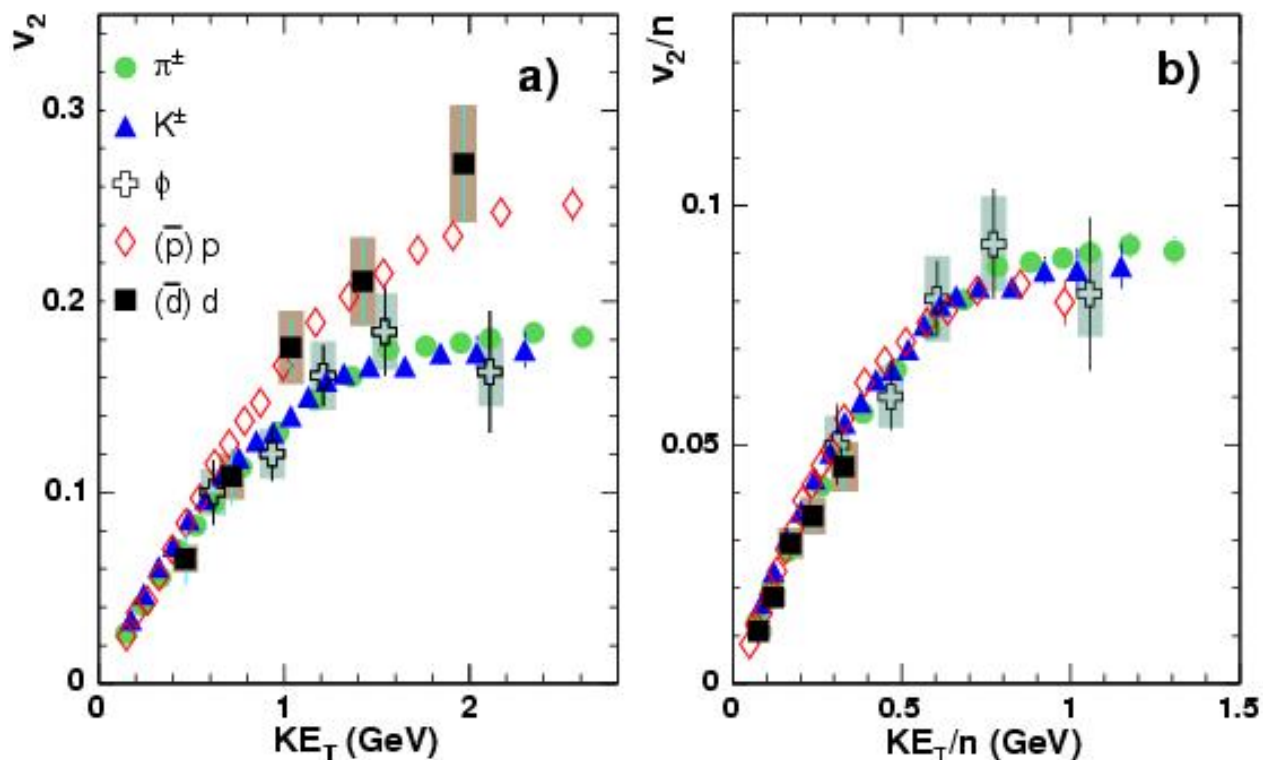
Universal scaling observed when:

- at low  $p_T$  when using the transverse kinetic energy  $KE_T = m_T - m$  in place of  $p_T$
- at high  $p_T$  when dividing both axis by the number of constituent quarks  $n_q$

**Indication that the  $v_2$  develops at a pre-hadronic stage**

# $\phi$ , $d$ and $\bar{d}$

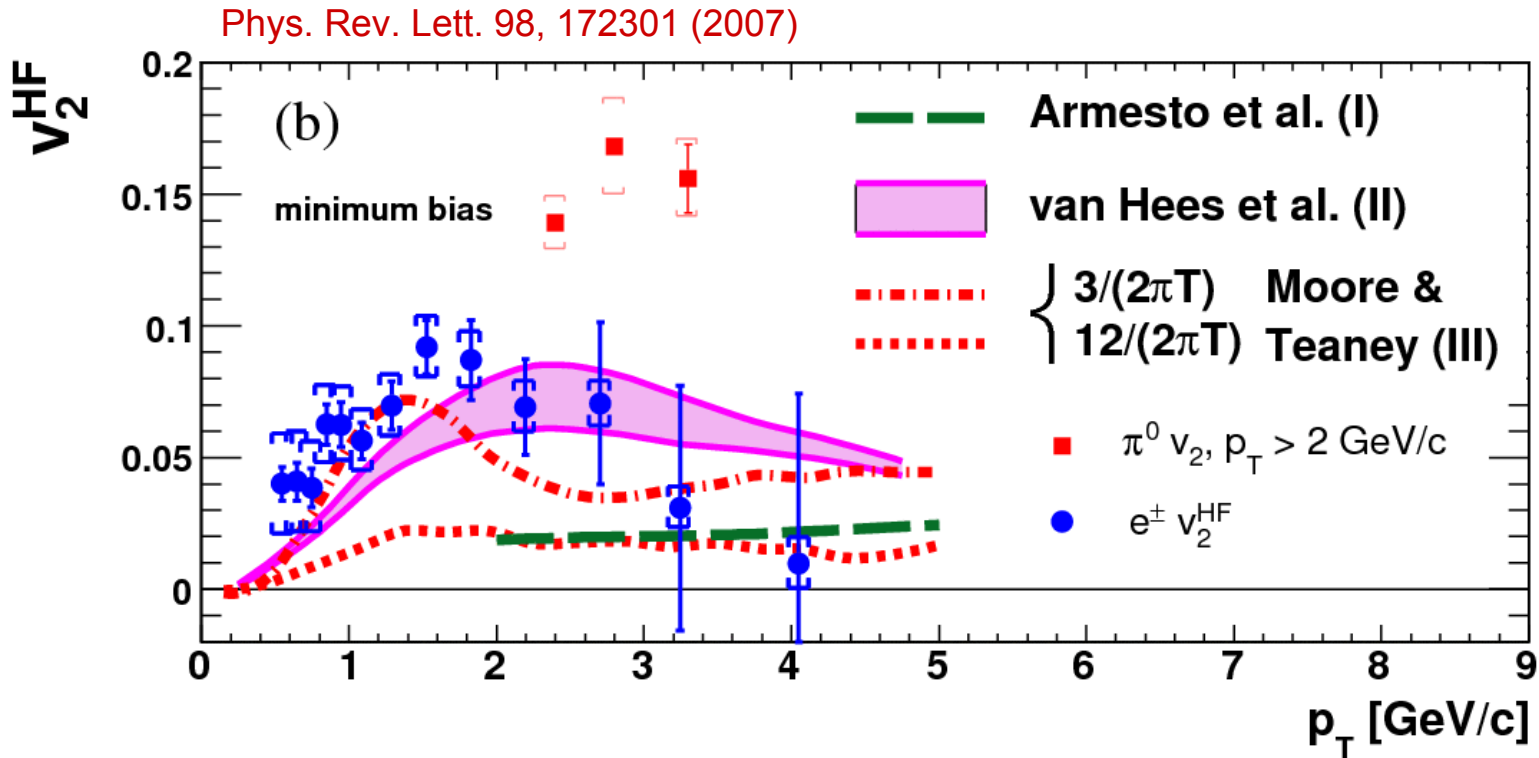
nucl-ex/0703024



- $\phi$  mesons have small hadronic cross-sections, but fall on the same curve.
- $d$  and  $\bar{d}$  also follow the same trend (although in a limited  $KE_T/n_q$  range), with  $n_q = 6$ .

**Indication that the  $v_2$  develops at a pre-hadronic stage**

# Heavy quarks



Sizeable  $v_2$  indicates strong coupling of charm to the medium.

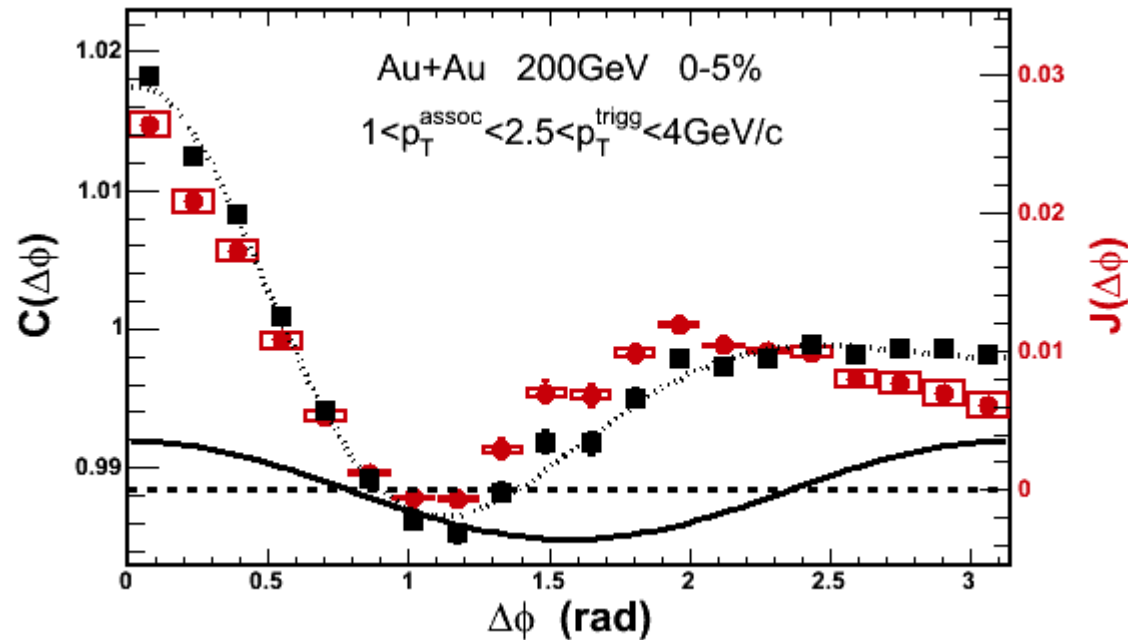
Presented calculations attempt to describe simultaneously charm  $R_{AA}$  and  $v_2$ .

They favor small charm relaxation time in medium and small viscosity for the surrounding medium, consistent with estimates from light hadrons measurements.

# Jet correlations

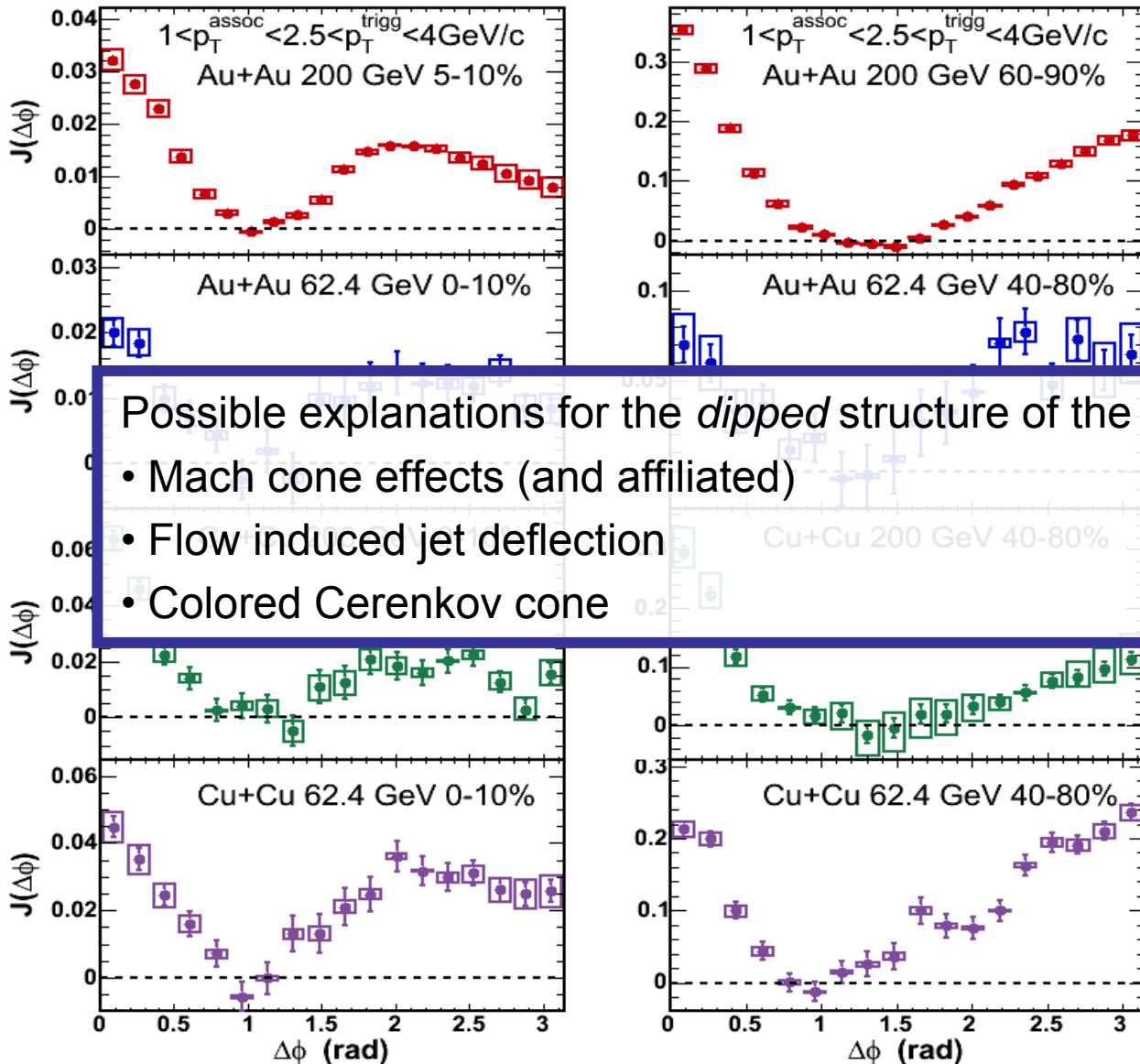
# Jet correlations (principle)

Jet correlation functions are derived from raw azimuthal correlations between a trigger particle of high  $p_T$  and same event associate particles, divided by the acceptance using event-mixing subtracted by the underlying event  $v_2$  contribution.



black is acceptance corrected correlation function.  
solid line is the  $v_2$  contribution.  
red is  $v_2$  subtracted correlation function (using ZYAM method).

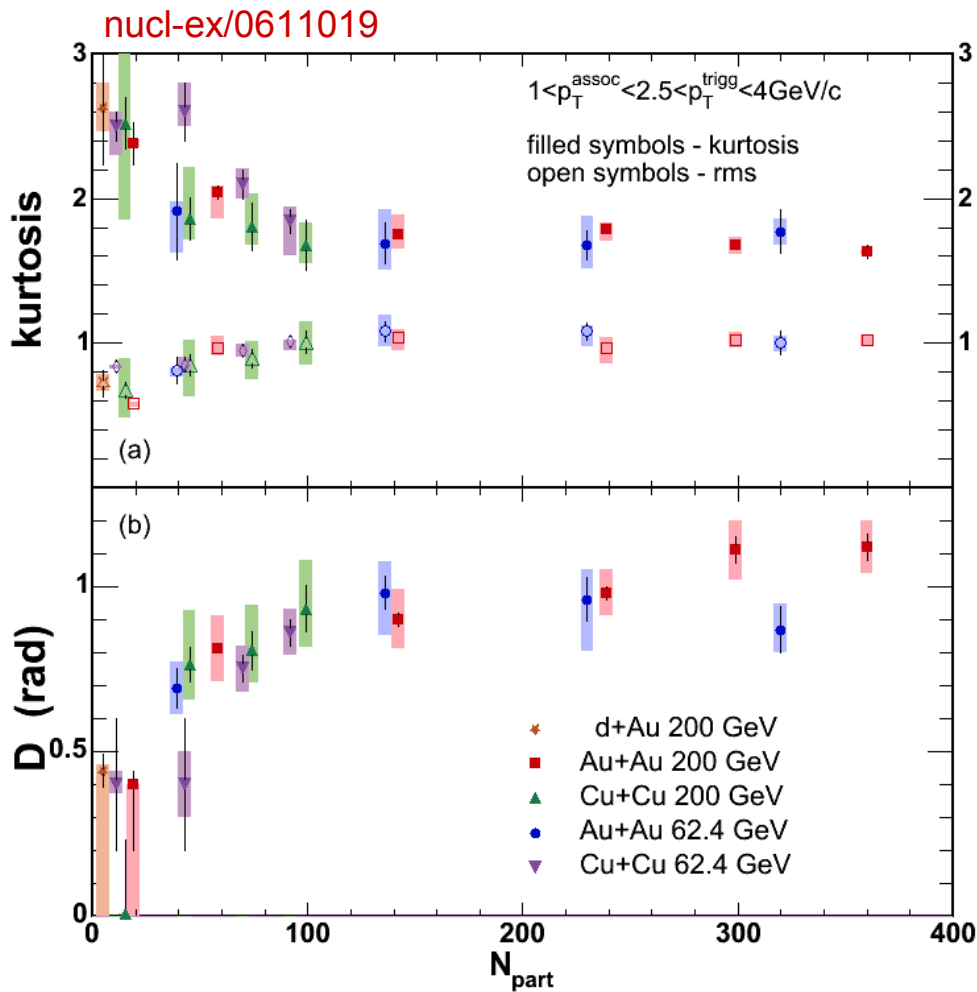
# Away side jet modification vs system and energy



Possible explanations for the *dipped* structure of the away side jet include:

- Mach cone effects (and affiliated)
- Flow induced jet deflection
- Colored Cerenkov cone

# Away side jet modifications vs system and energy



Here the shape of the away-side peak is characterized using 3 variables:

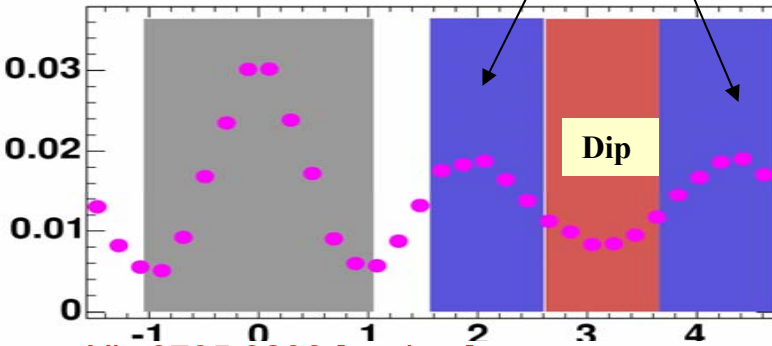
- RMS
- Kurtosis (=3 for Gaussian)
- D, distance between the peak and the local minimum, at  $\Delta\phi = \pi$

The broadening and peak location are found to depend on  $N_{\text{part}}$ , but not on the collision energy or colliding nuclei.

It is also independent of  $p_T^{\text{assoc}}$  (not shown here).

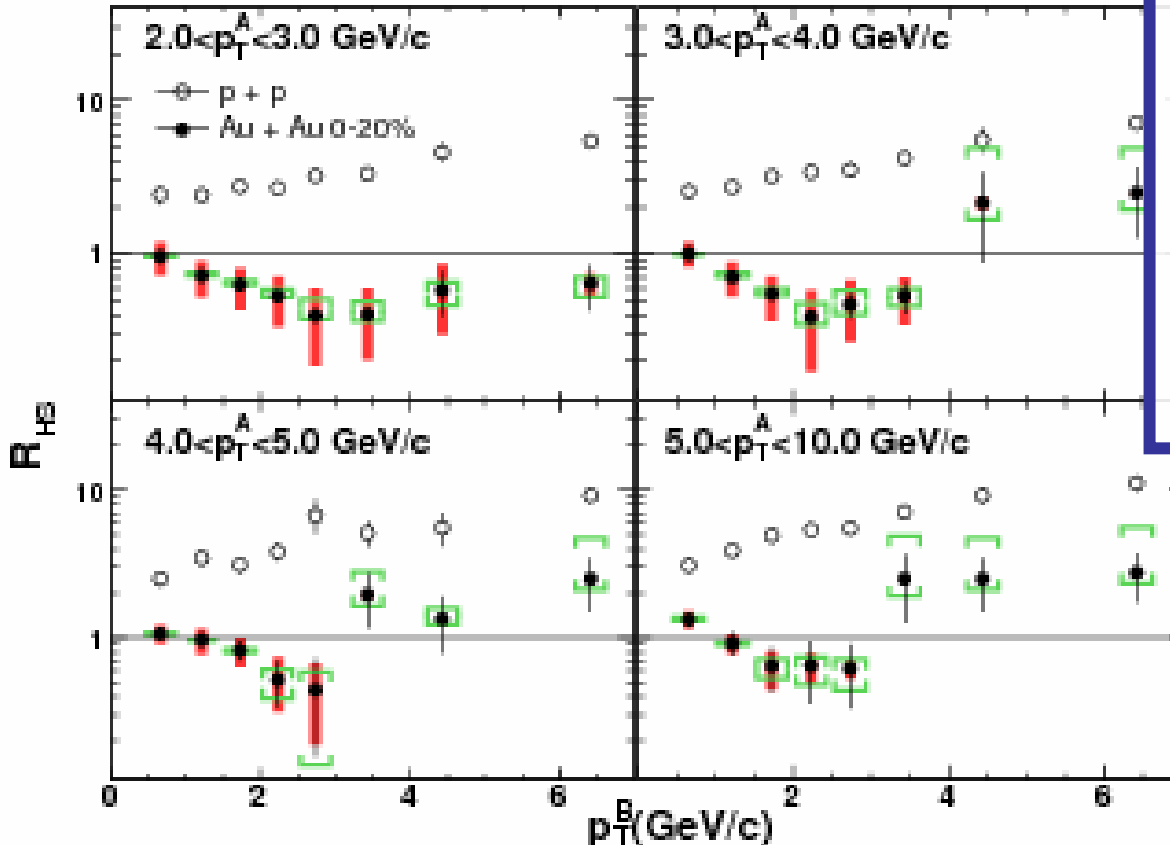
# Away side jet modifications vs $p_T^{\text{trig}} \times p_T^{\text{assoc}}$

Shoulder



Here the shape of the away-side peak is characterized using the ratio  $R_{\text{HS}}$  between the integral in the *head* region over the integral in the *shoulder* region

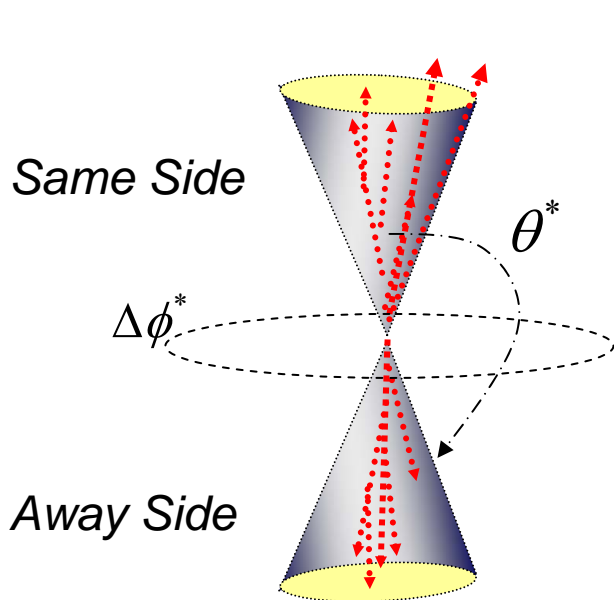
arXiv:0705.3238 [nucl-ex]



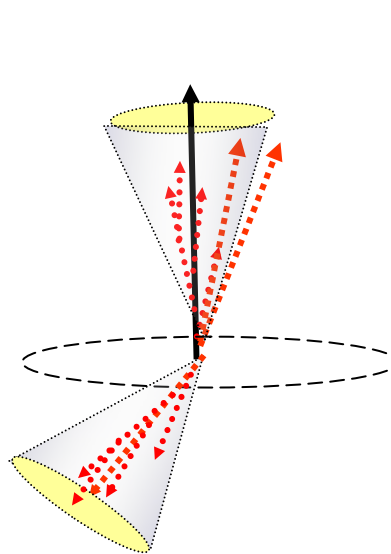
$R_{\text{HS}} < 1$  for small  $P_T^A \times P_T^B$  are representative of the dip at  $\Delta\phi = \pi$ .

$R_{\text{HS}} > 1$  for large  $P_T^A \times P_T^B$  are interpreted as a *re-appearance* of the away side peak, possibly due to *punch-through* jets

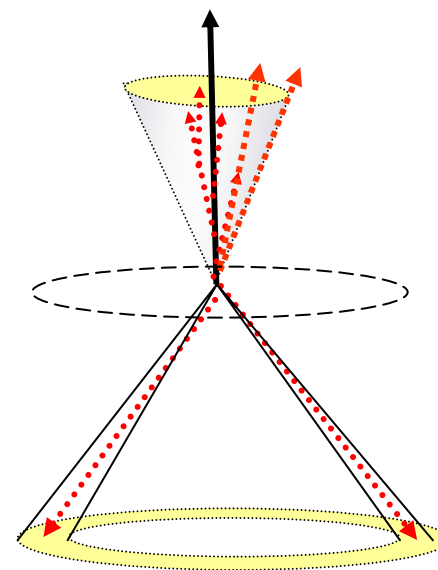
# Three particles correlations (principle)



Normal jet simulations



Deflected jet simulations



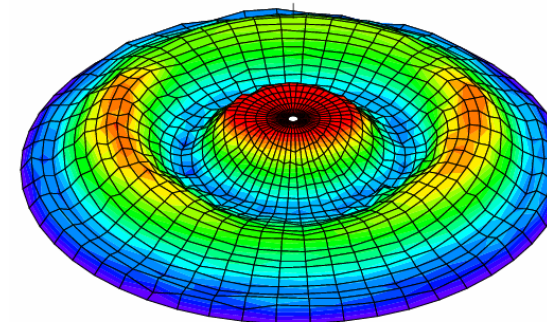
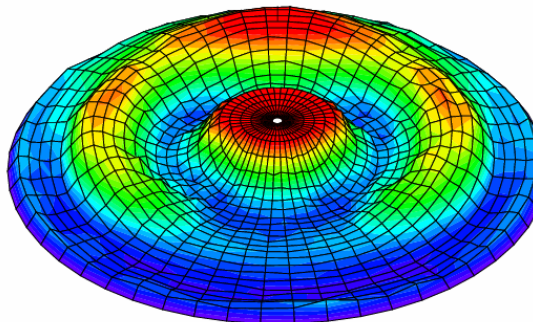
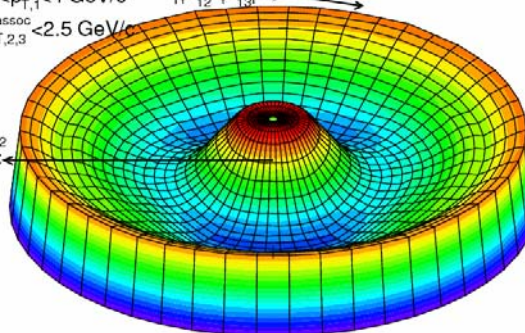
Mach Cone simulations

SIM Normal Jet Correlation PHENIX Acceptance

$2.5 < p_{T,1}^{\text{trig}} < 4 \text{ GeV}/c$   $|\phi_{12}^* - \phi_{13}^*| = 0$

$1 < p_{T,2,3}^{\text{assoc}} < 2.5 \text{ GeV}/c$

$\theta_{12}^* = \pi$

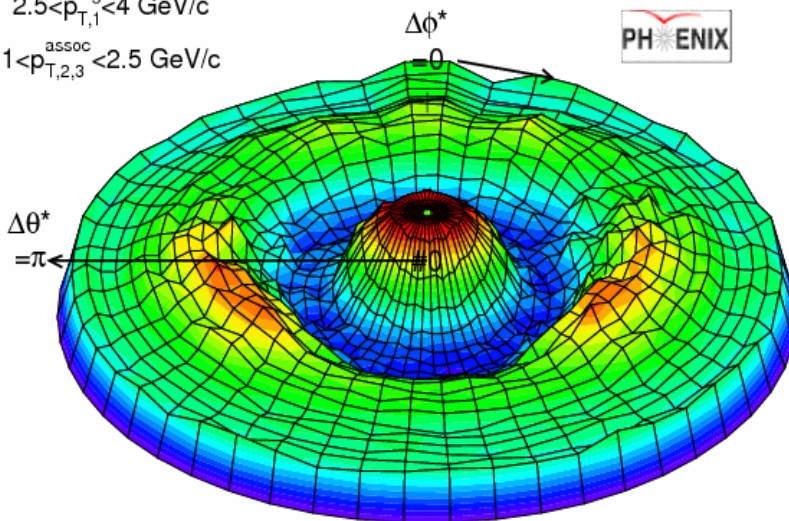


# Three particles correlations (data)

$\sqrt{s_{NN}}=200\text{GeV}$  PHENIX Total 3-Particle Jet Corrln. Cent = 10-20%

$2.5 < p_{T,1}^{\text{trig}} < 4 \text{ GeV}/c$

$1 < p_{T,2,3}^{\text{assoc}} < 2.5 \text{ GeV}/c$



PHENIX Preliminary

Associate particle yield variation along  $\Delta\Phi$

Blue is for deflected jets simulations

Red is for Mach cone effects

Data favor a Mach cone like structure but underlying  $v_2$  contribution is not subtracted.

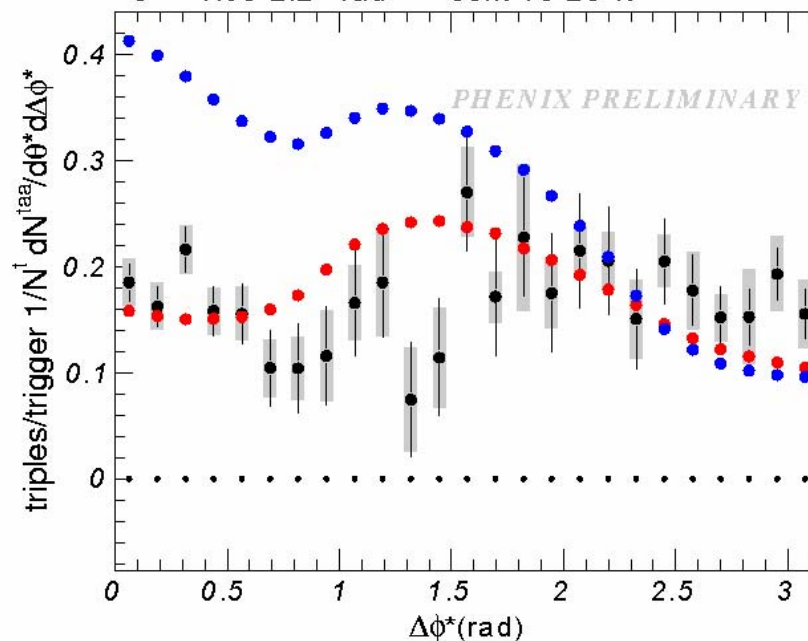


Au+Au  $\sqrt{s_{NN}}=200 \text{ GeV}$

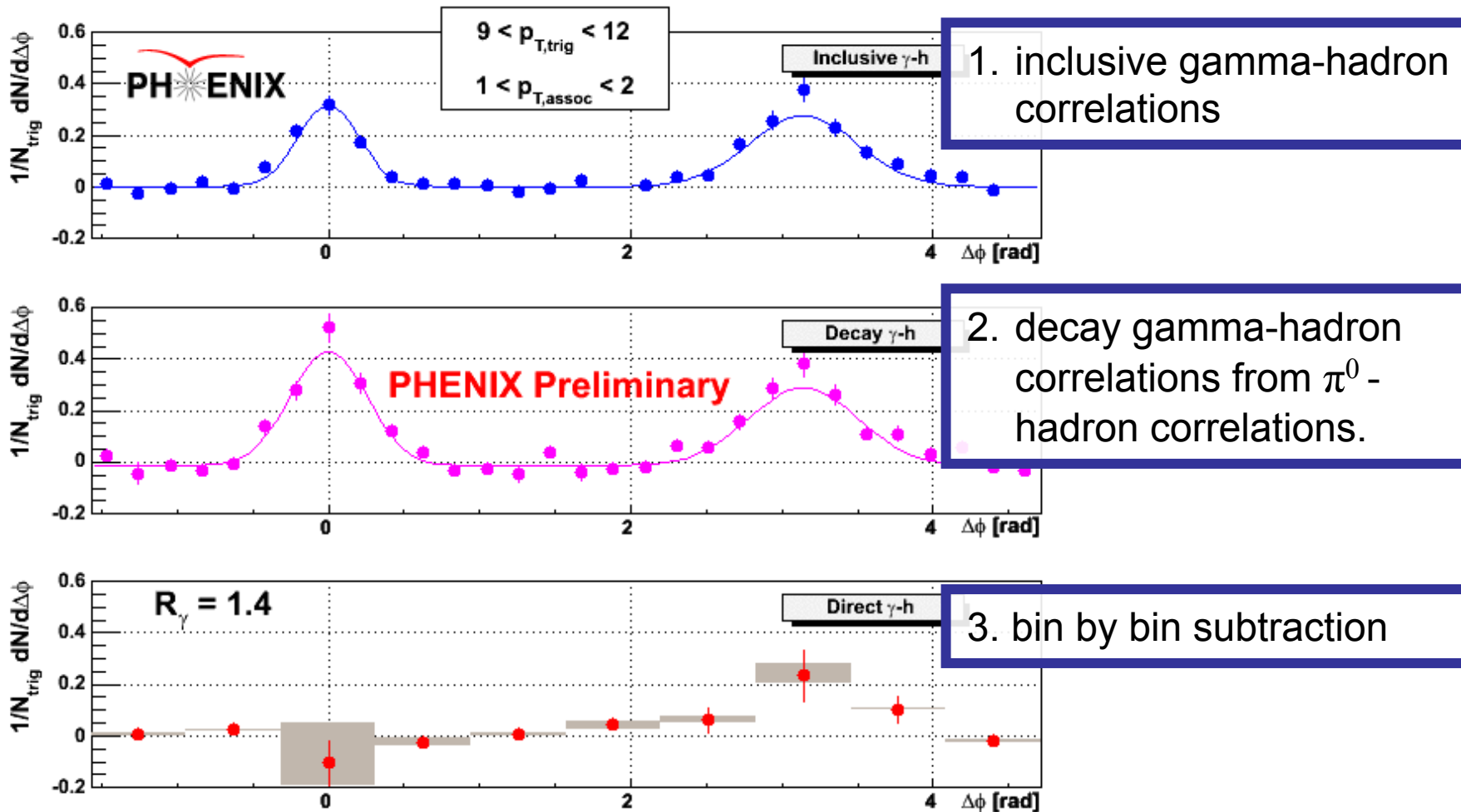
PHENIX  $\eta$  True 3-Particle Jet Correlation along  $\Delta\phi^*$

$2.5 < p_{T,1}^{\text{trig}} < 4 \text{ GeV}/c$   $1 < p_{T,2,3}^{\text{assoc}} < 2.5 \text{ GeV}/c$

$\theta^* = \langle 1.65 - 2.2 \rangle \text{ rad}$  cent 10-20 %

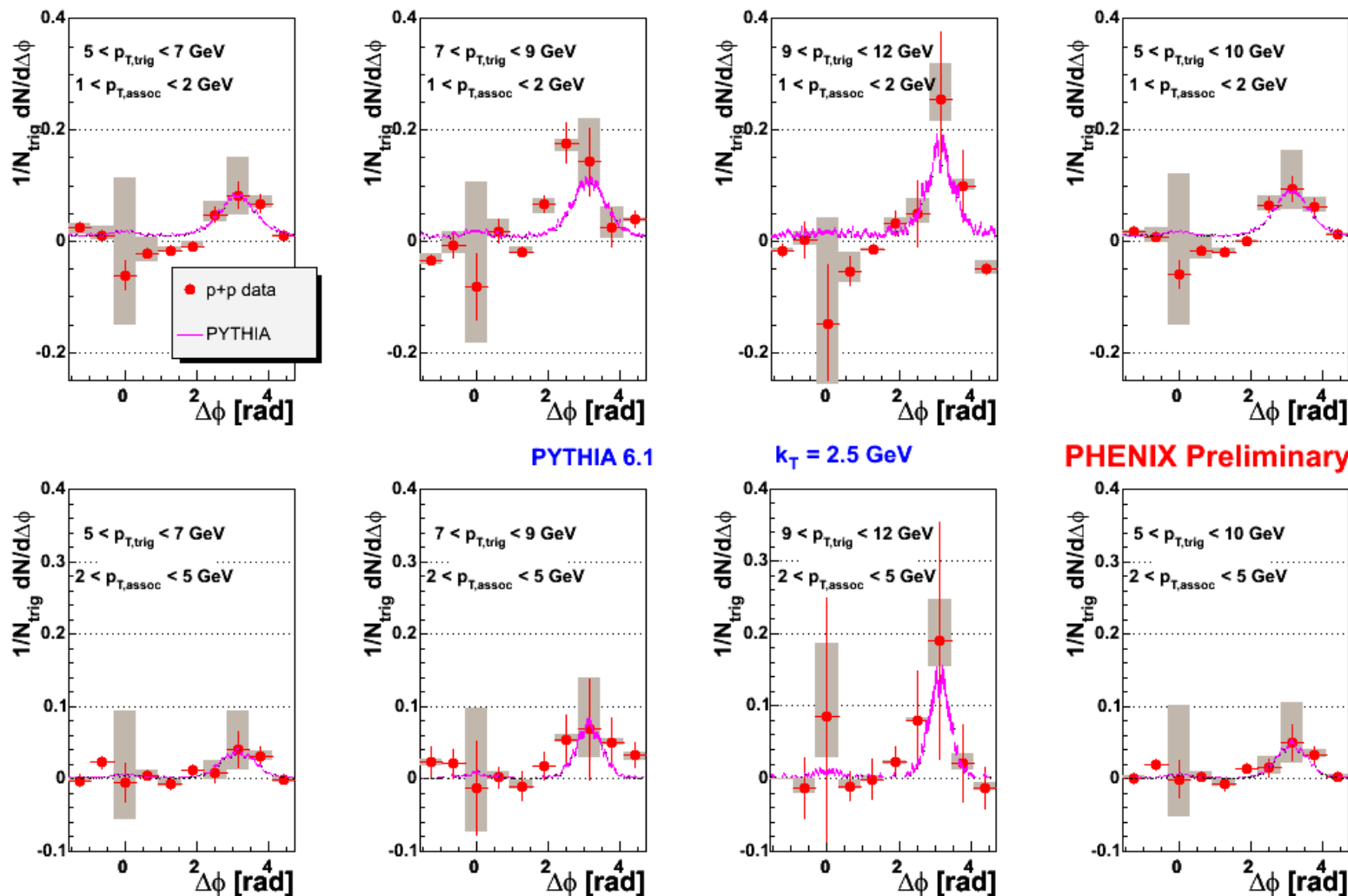


# Gamma - jet correlations (principle)



As a cross-check, near side peak should cancel because direct photons are isolated (at first order). This validates the accuracy of the subtraction.

# Gamma - jet correlations in p+p

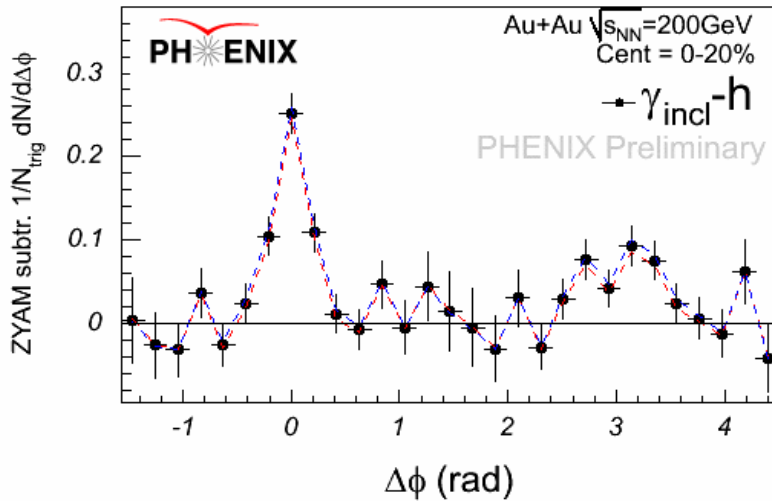


Comparison between p+p direct photon-hadron correlations and pythia.  
Good agreement achieved although large error bars.

# Gamma - jet correlations in Au+Au

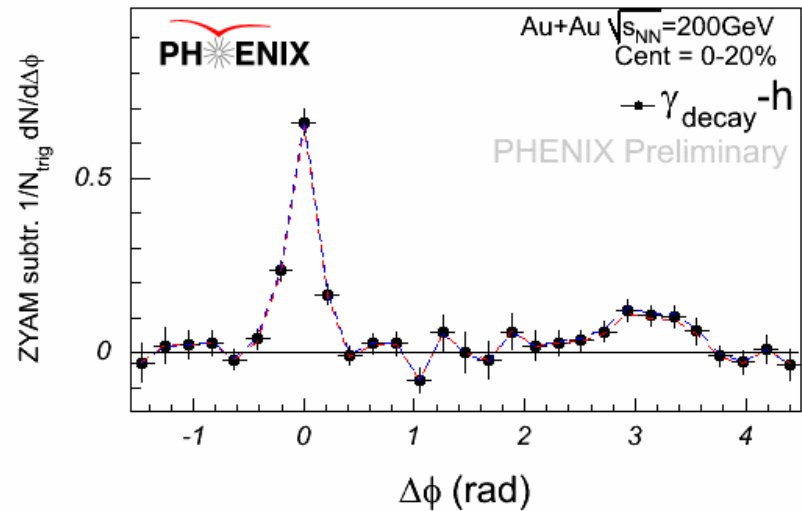
## inclusive photon - hadron

associated  $h^{+/-}$   $p_T \in [2,5]$  GeV/c, trigger  $p_T \in [7,9]$  GeV/c



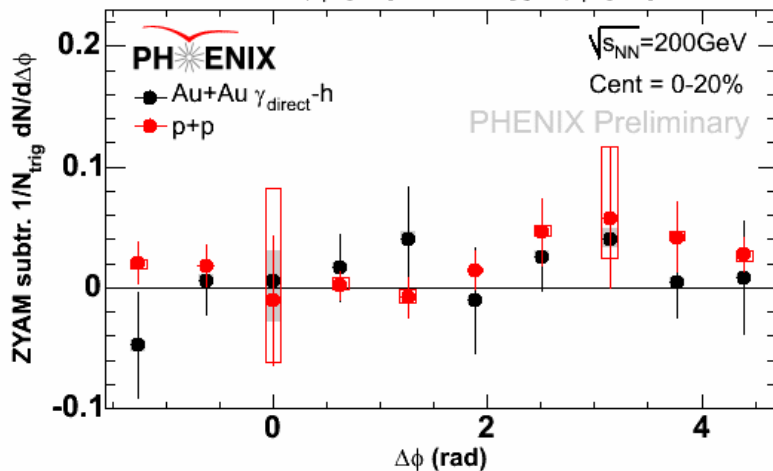
## decay photon - hadron

associated  $h^{+/-}$   $p_T \in [2,5]$  GeV/c, trigger  $p_T \in [7,9]$  GeV/c

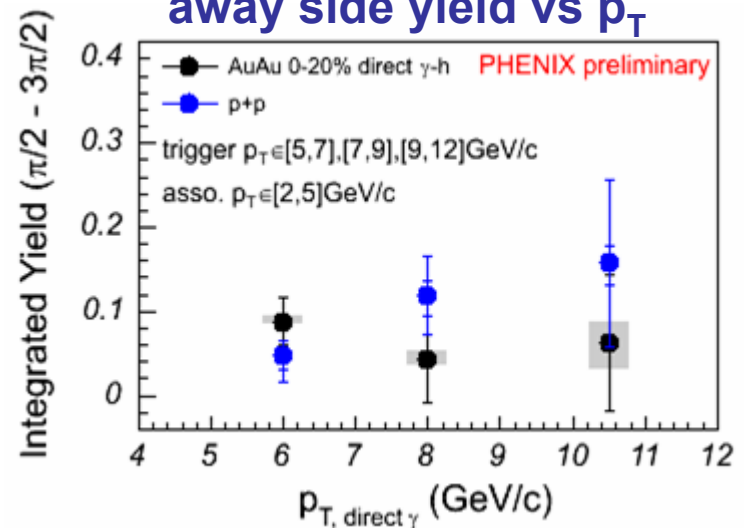


## direct photon - hadron

associated  $h^{+/-}$   $p_T \in [2,5]$  GeV/c, trigger  $p_T \in [7,9]$  GeV/c



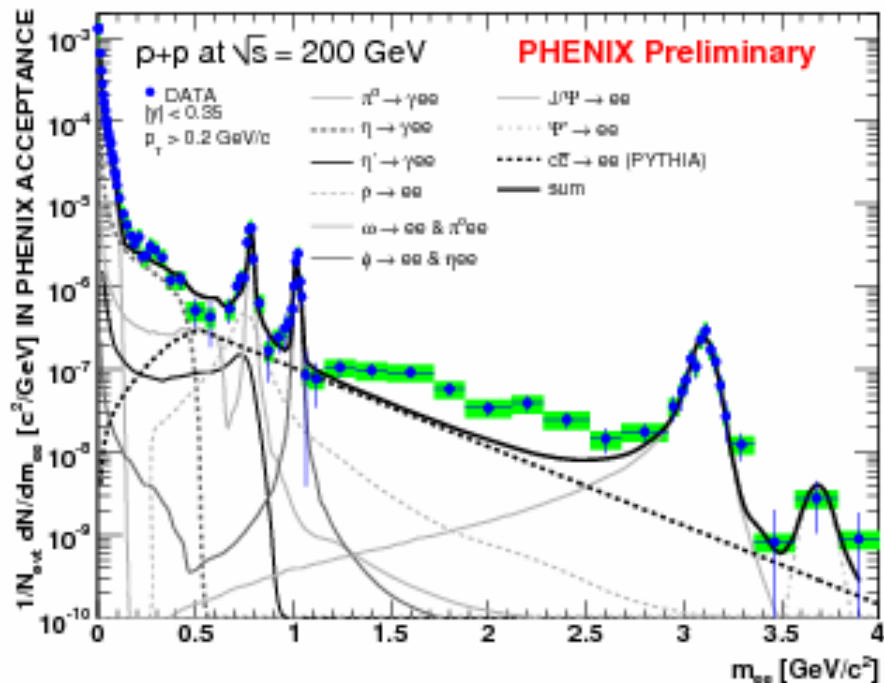
## away side yield vs $p_T$



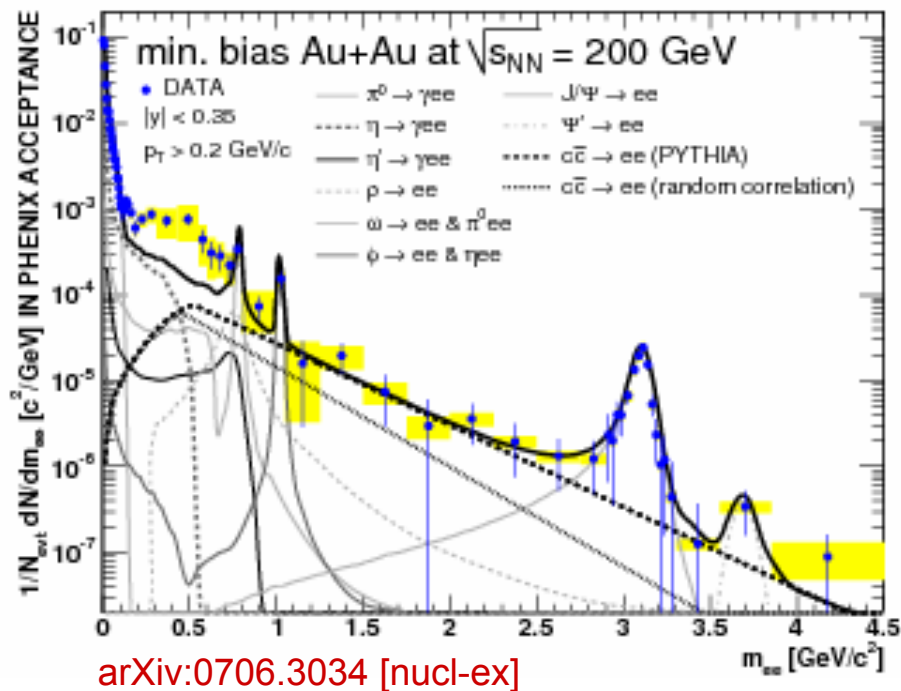
# di-lepton continuum and heavy quarkonia

# di-electron invariant mass distribution

p+p

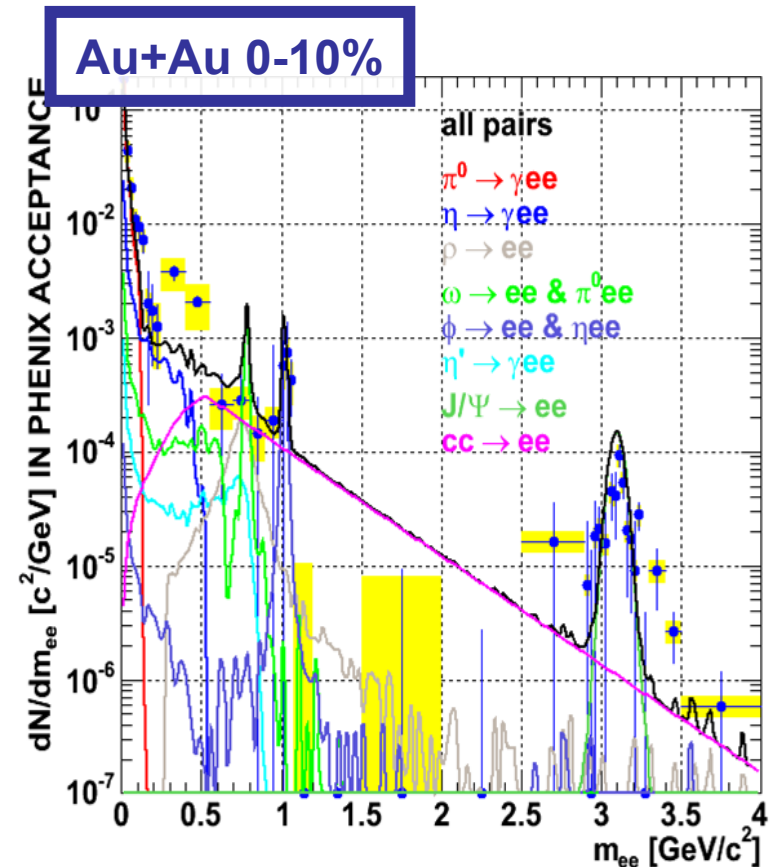
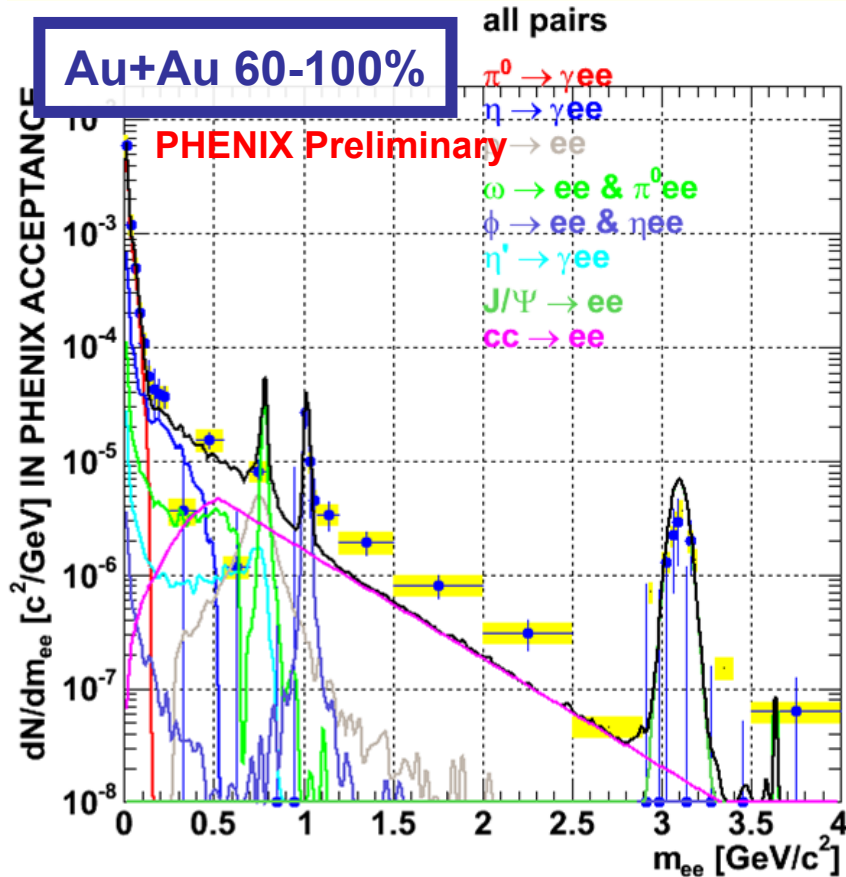


Au+Au minimum bias



A significant excess is observed at low mass ( $m < 1$  GeV/c) in Au+Au minimum bias

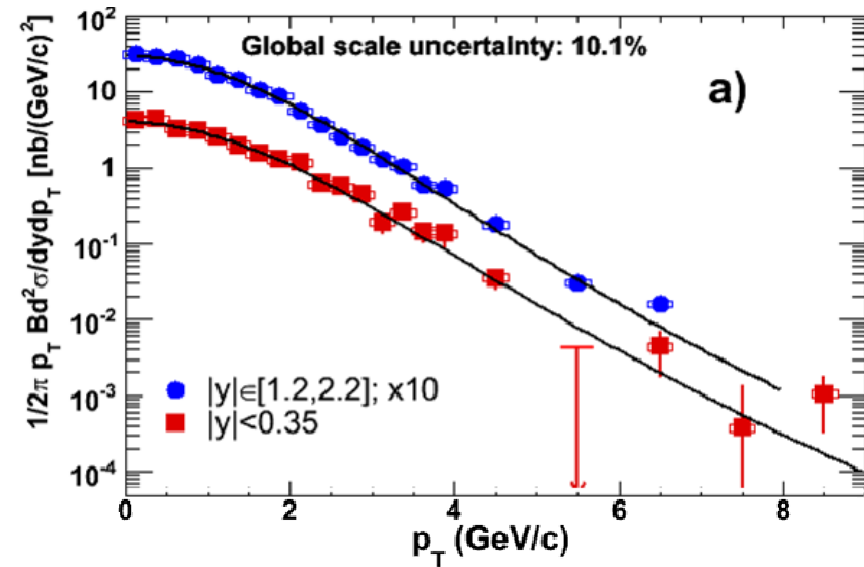
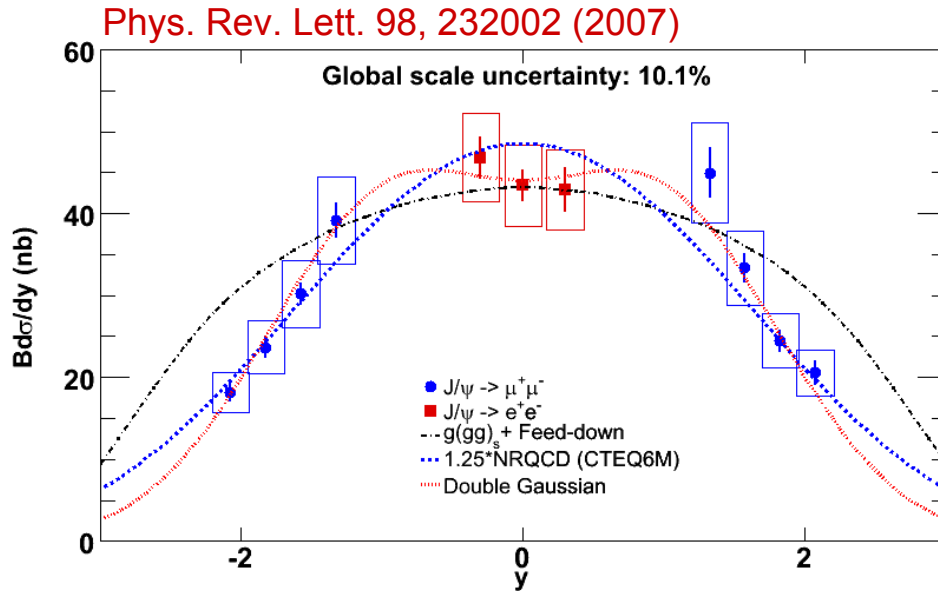
# di-electron invariant mass distribution centrality dependence



Au+Au peripheral behaves essentially like p+p

Au+Au central: excess at low mass ( $m < 1 \text{ GeV}/c$ ) as for minimum bias.

# J/Ψ production in p+p collisions

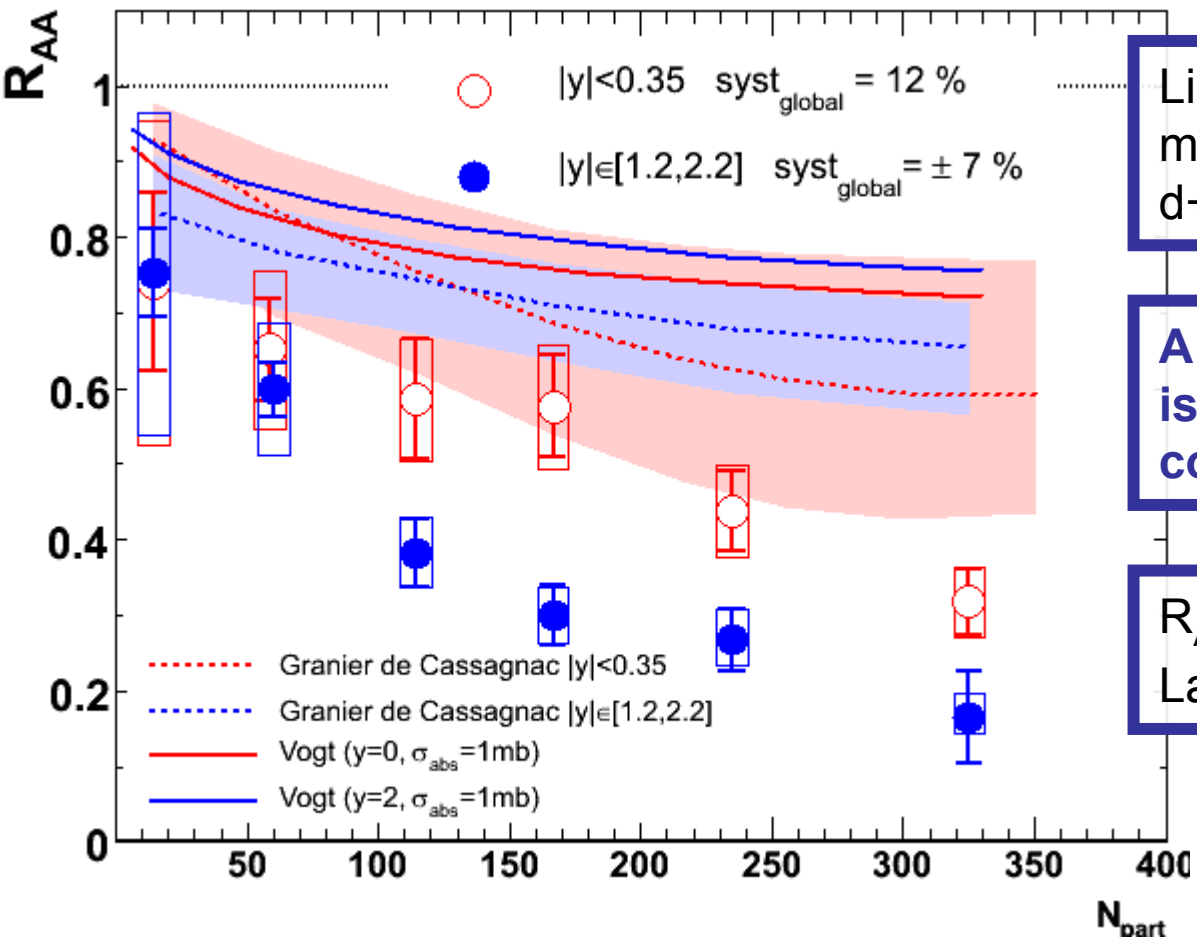


**10 times more statistics as previous measurement.**

- better constraints on rapidity and  $p_T$  spectrum
- better reference for the nuclear modification factor

# J/Ψ R<sub>AA</sub> in Au+Au

Phys. Rev. Lett. 98, 232001 (2007)

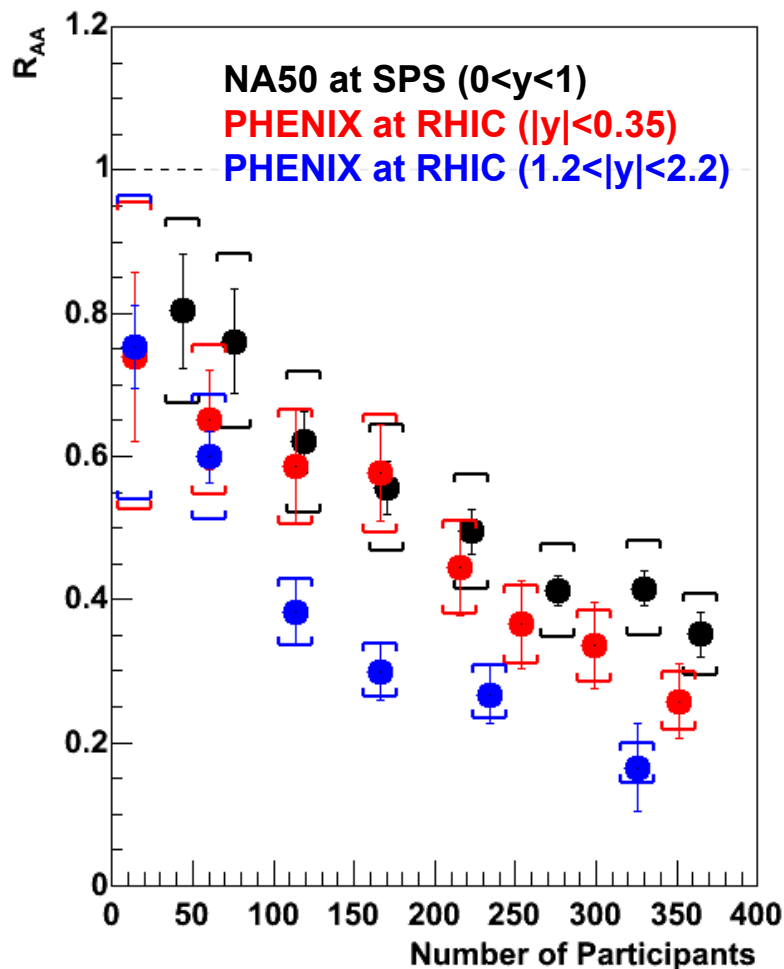


Lines + bands are cold nuclear matter effects, extrapolated from d+Au

A suppression is observed that is beyond extrapolations from cold nuclear matter effects

$R_{AA} \sim 0.3$  for central collisions  
Larger suppression at  $|y| > 1.2$

# Comparison to SPS



At mid-rapidity, suppression at RHIC is similar to SPS, but:

- cold nuclear matter effects are larger at SPS
- energy density is larger at RHIC

At RHIC there is more suppression at forward rapidity than at mid rapidity. Unexpected because energy density is larger at mid-rapidity.

**Indications that more complex mechanism must be involved than energy density driven suppression.**

## Additional topics covered during this conference

- 3D two-pions source imaging (P. Chung Wednesday, June 27)
- Longitudinal density correlations (T. Nakamura, Monday June 25)

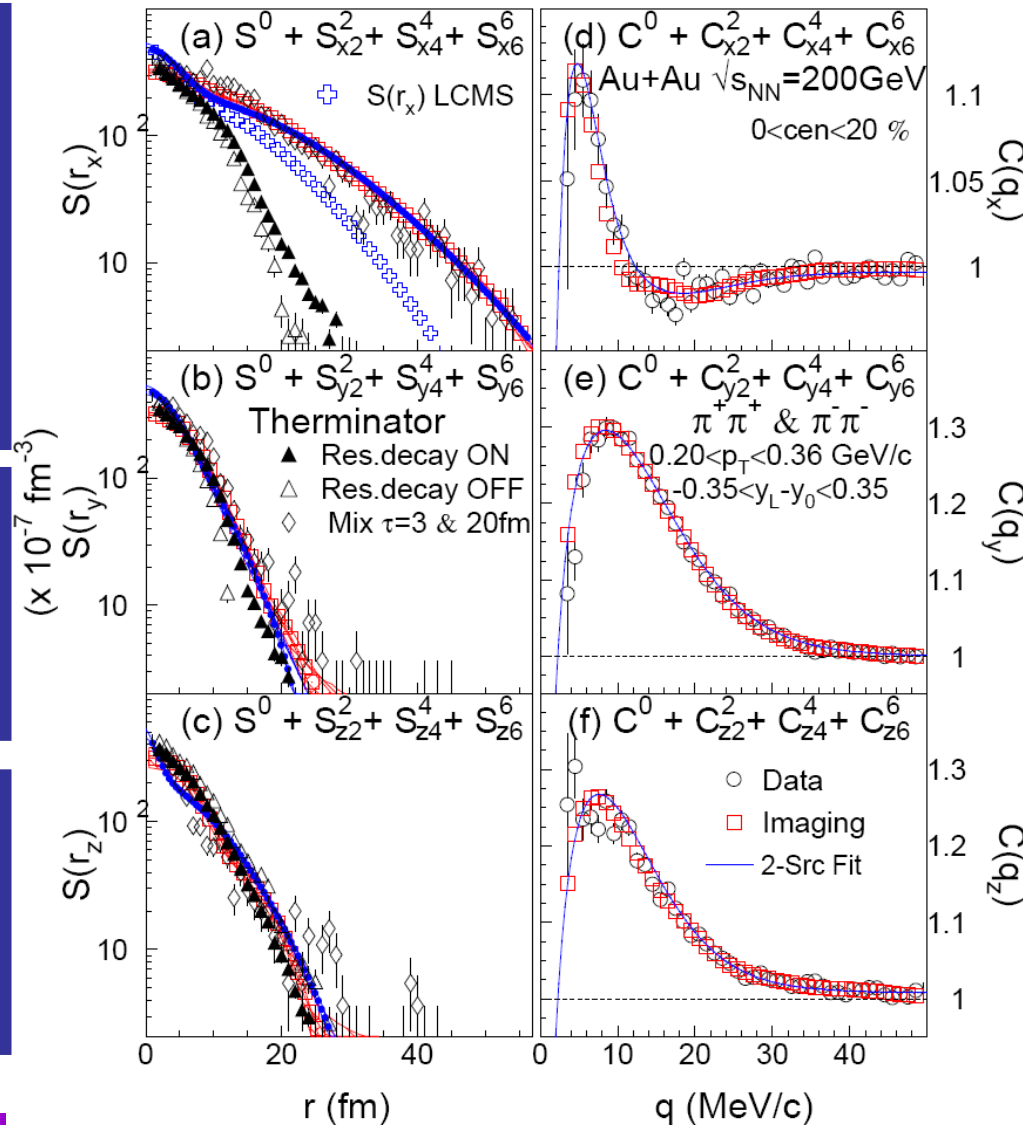
# 3D two-pions source imaging

Look at 2-pions correlation functions in 3D space; extract 3D cartesian moments of the observed distributions, and from there the 2-pions source functions  $S(r)$ :  
**probability to emit a pair of pions at a separation  $r$  in the pair rest frame**

Source functions describe how pions are produced during hadronization and carry information about the phase transition.

**Long range source term along  $x$  (parallel to the pair  $P_T$ ), can be modeled by adding a delayed pion source emission.**

phenix preliminary

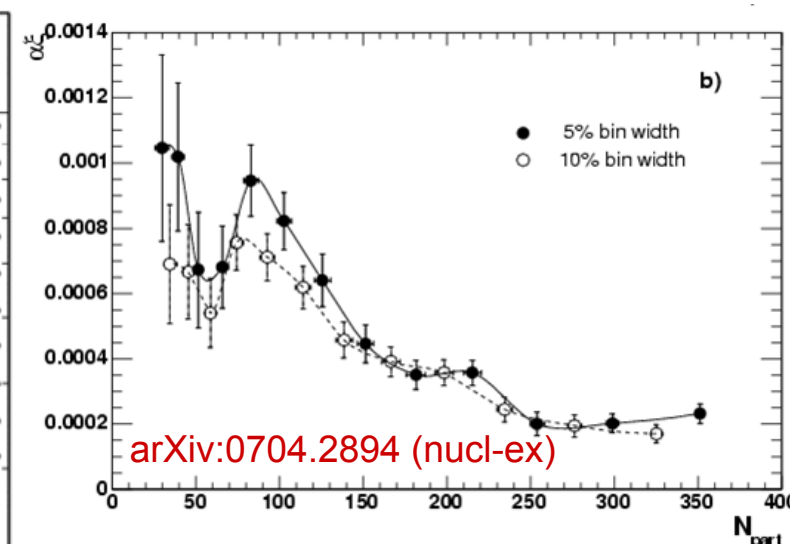
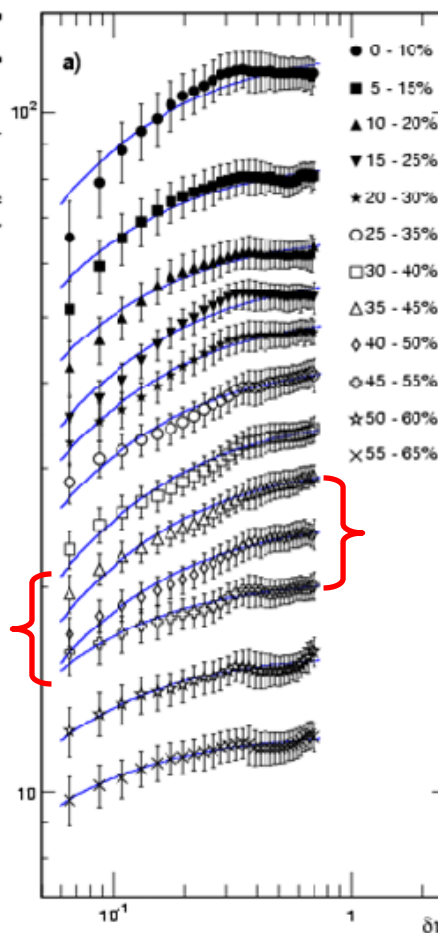
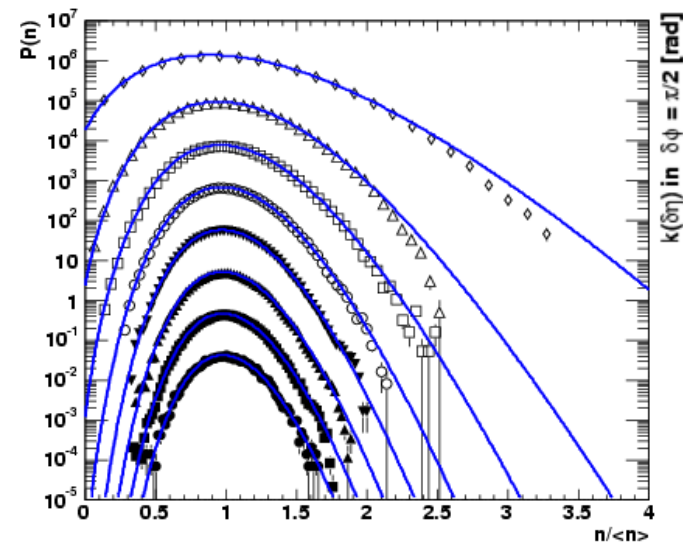


# Longitudinal density correlations

1 Fit event/event multiplicity fluctuation vs rapidity domain and centrality with negative binomial distribution (NBD)

2 fit  $k(\delta\eta)$ , characteristic of the width of the NBD to extract  $\alpha\xi$ , a parameter monotonically related to the medium **susceptibility**

3 look at  $\alpha\xi$  vs  $N_{\text{part}}$



Talk: T. Nakamura,  
Monday June 25

The non monotonic behavior  $\alpha\xi$  around  $N_{\text{part}} \sim 90$  could indicate critical behavior at a phase boundary.

# Conclusions

The matter created in heavy ions collisions at RHIC is dense enough to suppress light hadrons up to very high  $p_T$  as well as charmed mesons. Data favor high opacity of the medium, high gluon density and low viscosity.

It strongly affects the jet structure. Data favor Mach cone like deformations (as opposed to deflected jets).

Scaling properties of the elliptic flow indicate that it would form prior to hadronization, meaning that the system is thermalized while still in a partonic phase.

As was originally predicted,  $J/\Psi$  is suppressed in the medium, however the picture is more complex than expected.

# Back-up

# BNL Facility



**length:** 3.83 km

Capable of colliding  
*any* nuclear species

**Energy:**

500 GeV for p-p

200 GeV for Au-Au  
(per N-N collision)

**protons:** Linac → Booster → AGS → RHIC

**ions:** Tandems → Booster → AGS → RHIC

# Collision species and energy

Run	Year	Species	Energy (GeV)	# J/ $\Psi$ (ee+ $\mu\mu$ )
01	2000	Au+Au	130	0
02	2001/2002	Au+Au	200	13 + 0
		p+p	200	46 + 66
03	2002/2003	d+Au	200	360 + 1660
		p+p	200	130 + 450
04	2003/2004	Au+Au	200	~ 1000 + 5000
		Au+Au	62	13 + 0
05	2004/2005	Cu+Cu	200	~ 1000 + 10000
		Cu+Cu	62	10 + 200
		Cu+Cu	22.5	
		p+p	200	~ 1500 + 10000
06	2006	p+p	200	~ 3000 + 30000
		p+p	62	
		p+p	500	

# New detectors

## 2006

aerogel and time-of-flight system

hadron-blind detector

reaction plane detector

time of flight

forward electromagnetic calorimeter

## 2006 – 2009

Silicon vertex tracker

muon trigger

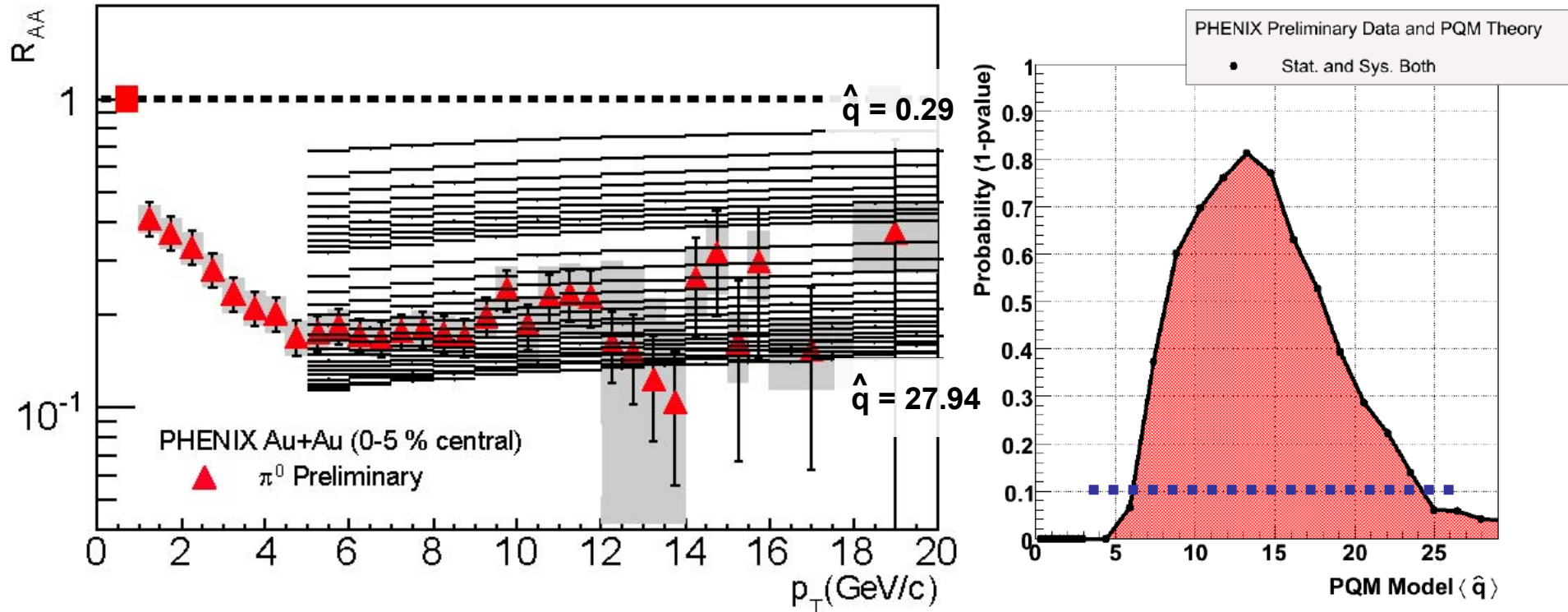
## 2008 – 2011

forward silicon vertex tracker

nose cone calorimeter

# Getting quantitative statements from $\pi^0 R_{AA}$

Comparison of measured  $\pi^0 R_{AA}$  to PQM energy loss predictions vs  $\hat{q}$



PQM - C. Loizides hep-ph/0608133v2:

$$6 \leq \hat{q} \leq 24 \text{ GeV}^2/\text{fm}$$

GLV - I. Vitev hep-ph/0603010:

$$1000 \leq dN_g/dy \leq 2000$$

WHDG - W. Horowitz:

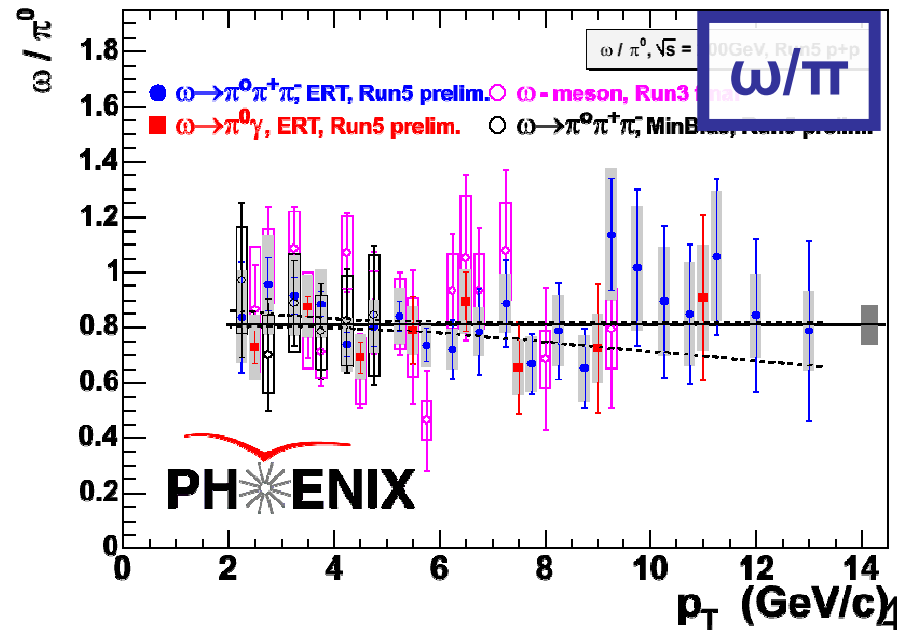
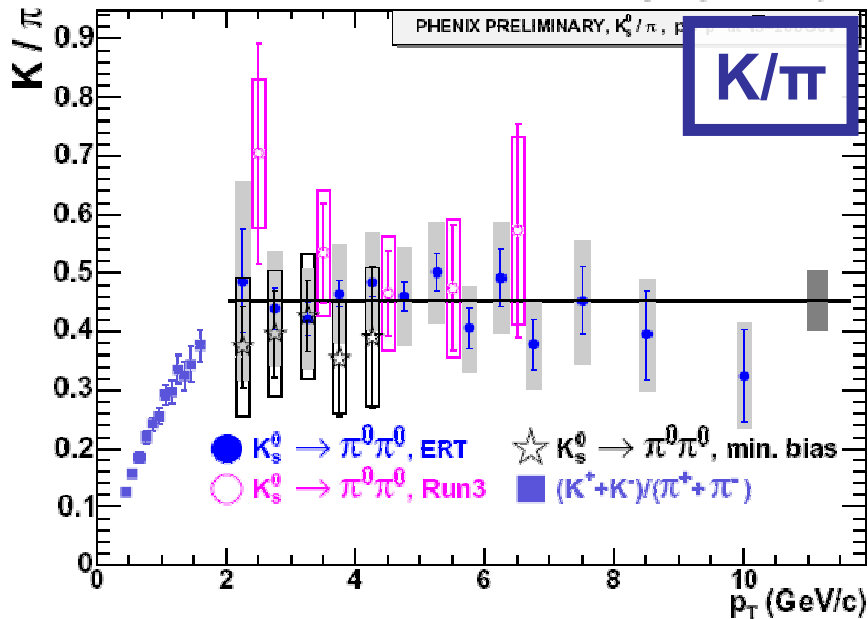
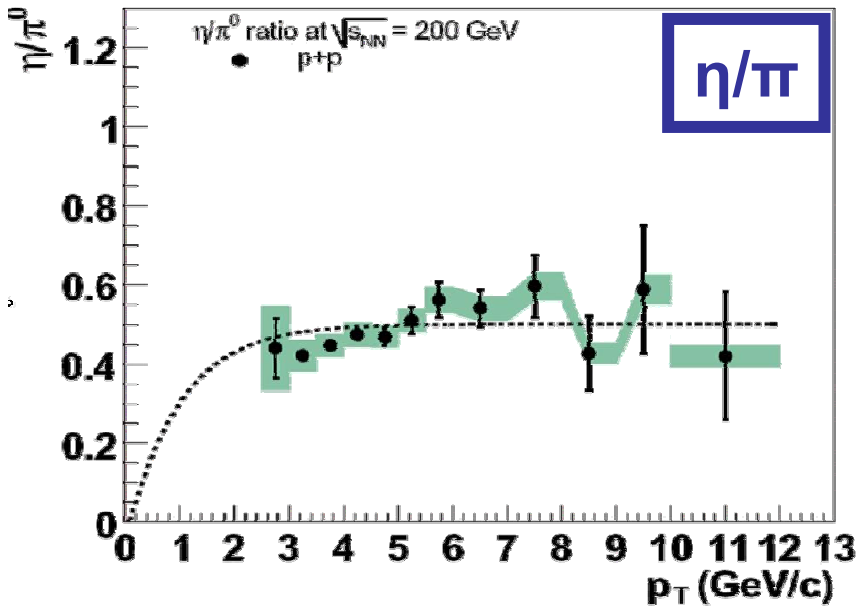
$$600 \leq dN_g/dy \leq 1600$$

# Light meson decay channels measured by PHENIX

## Light meson resonances

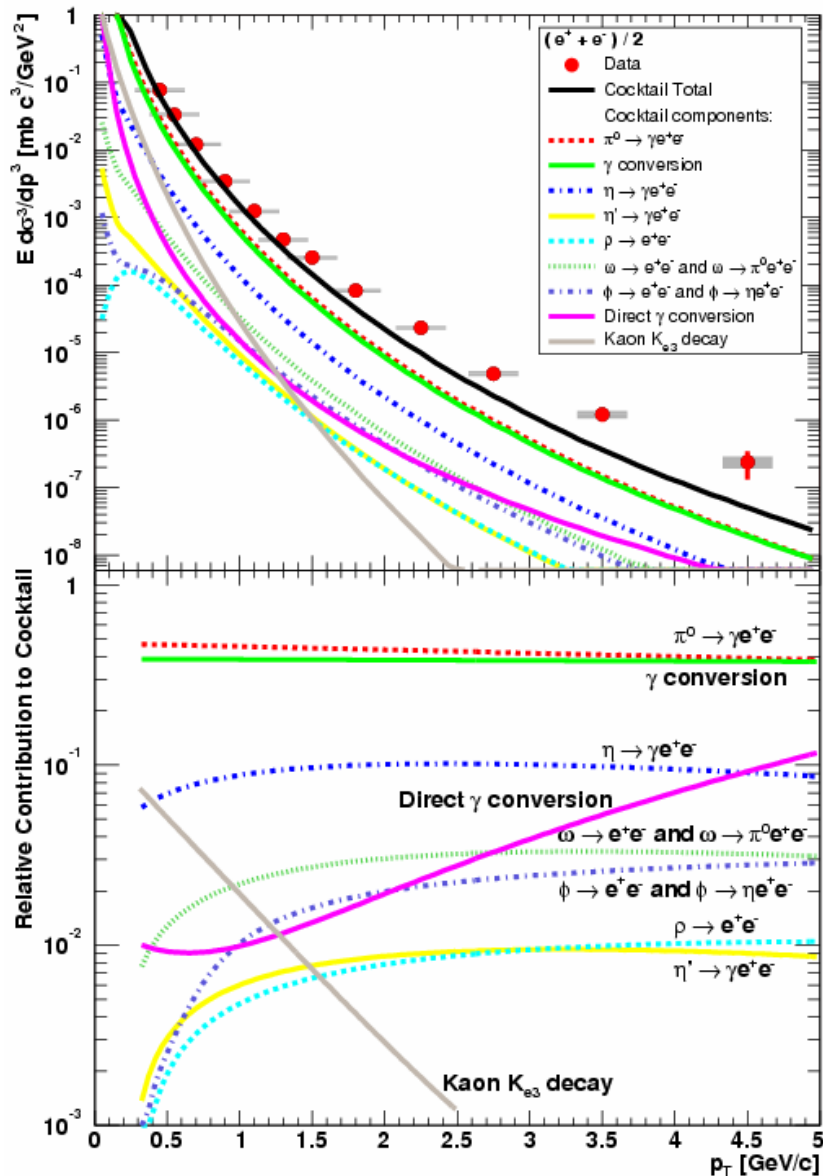
$\phi \rightarrow K^+K^-$	BR = $49.2 \pm 0.7\%$
$\phi \rightarrow e^+e^-$	BR = $2.97 \pm 0.04\%$
$\omega \rightarrow e^+e^-$	BR = $7.18 \pm 0.12\%$
$\omega \rightarrow \pi^0\gamma$	BR = $8.90 \pm 0.25\%$
$\omega \rightarrow \pi^0\pi^+\pi^-$	BR = $89.1 \pm 0.7\%$
$\eta \rightarrow \gamma\gamma$	BR = $39.39 \pm 0.24\%$
$\eta \rightarrow \pi^0\pi^+\pi^-$	BR = $22.68 \pm 0.35\%$
$K^S \rightarrow \pi^0\pi^0$	BR = $30.69 \pm 0.05\%$
$K^\pm$	using ToF

# Light mesons particle ratios



**Heavy flavor**

# Inclusive single electron spectrum and cocktail



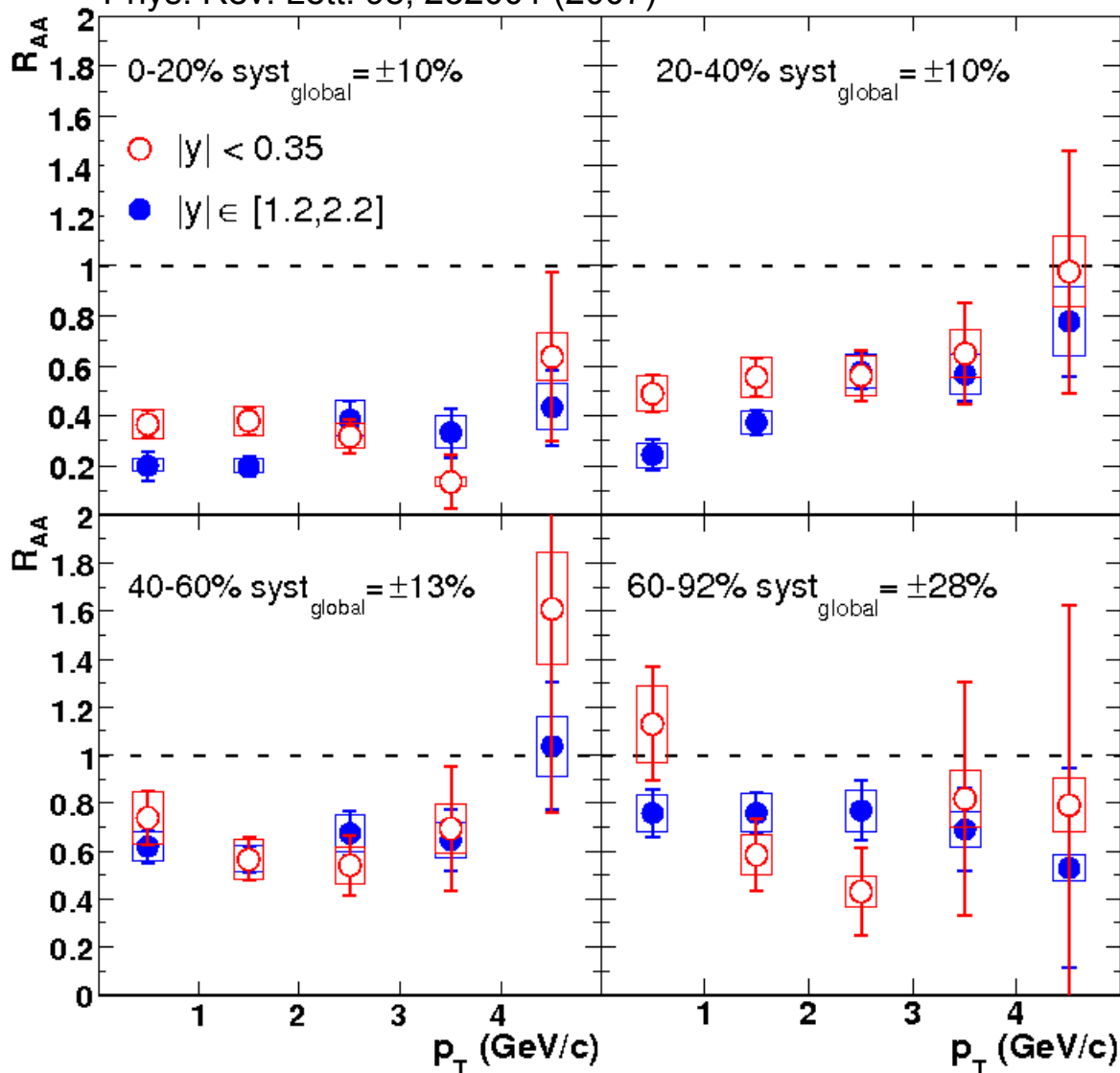
## Cocktail method (data driven simulations):

- $\pi$  contribution based on PHENIX measurements
- $\gamma$  conversion contribution from material budget
- light meson contributions from lower energy data and  $m_T$  scaling from  $\pi$  data

# Nuclear modification factor vs $p_T$ in Au+Au

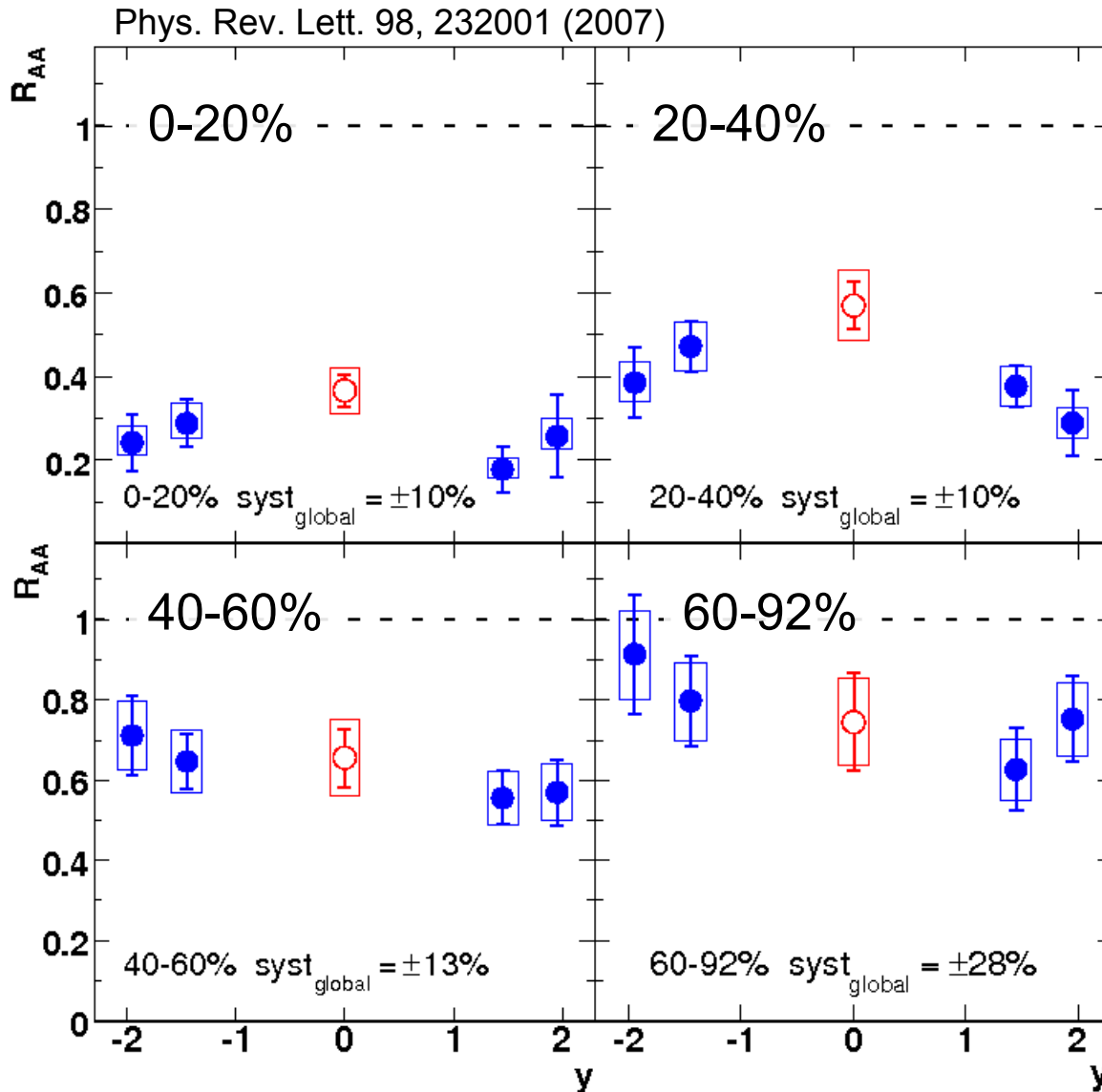
Measurement from 2004 Au+Au (nucl-ex/0611020)

Phys. Rev. Lett. 98, 232001 (2007)



No significant change of the  $p_T$  distributions with respect to p+p, but error bars are large

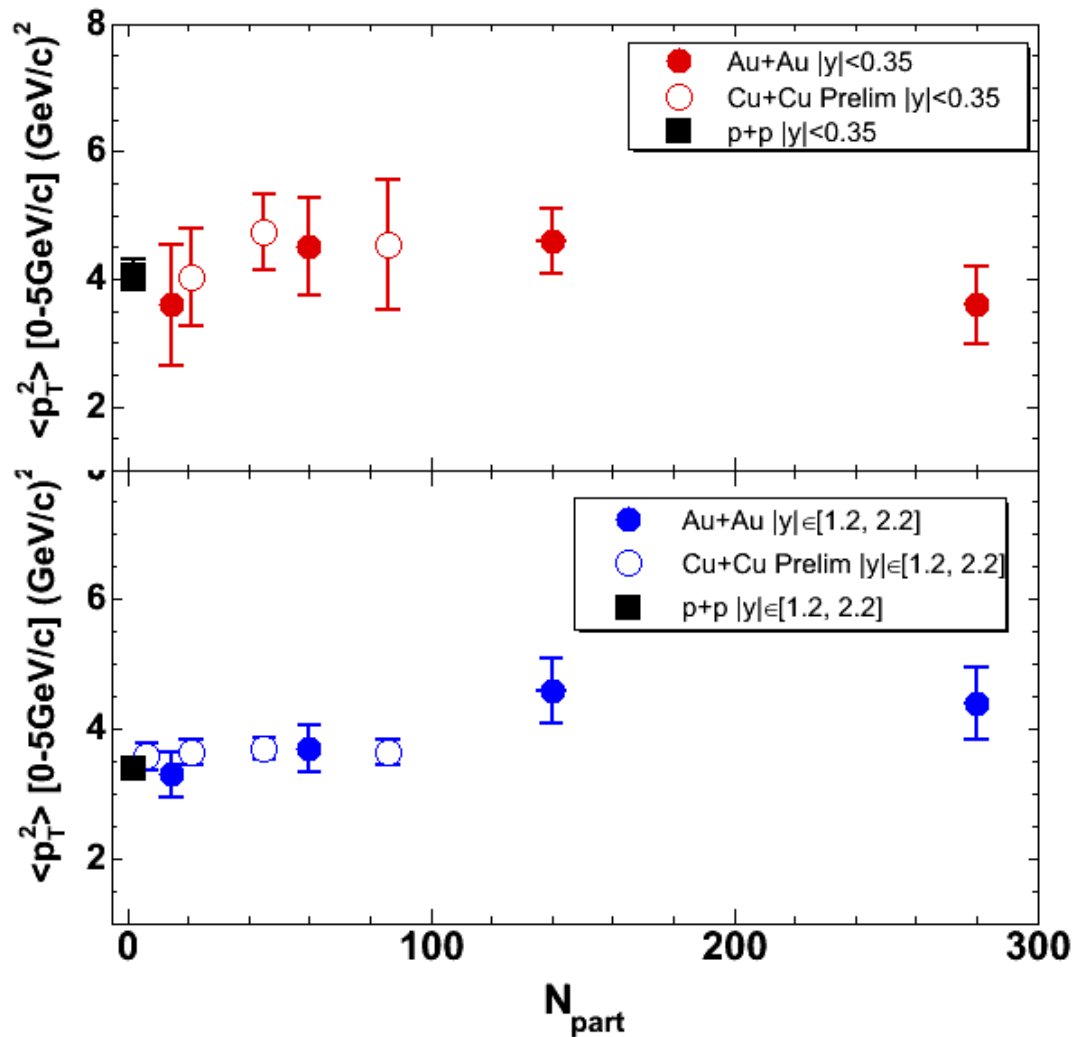
# $J/\Psi$ $R_{AA}$ vs rapidity in Au+Au



**Peripheral collisions:**  
no modification of the rapidity distribution with respect to p+p collisions

**Central collisions:**  
narrowing of the rapidity distribution

# Mean $p_T^2$ (truncated) vs $N_{part}$



$\langle p_T^2 \rangle$  (truncated to  $0 < p_T < 5 \text{ GeV}/c$ ) shows no significant variation vs  $N_{part}$  for all systems.

# Proton spin structure via heavy flavor

Proton spin structure is probed using longitudinally polarized proton beams. Beam polarization is flipped from bunch to bunch.

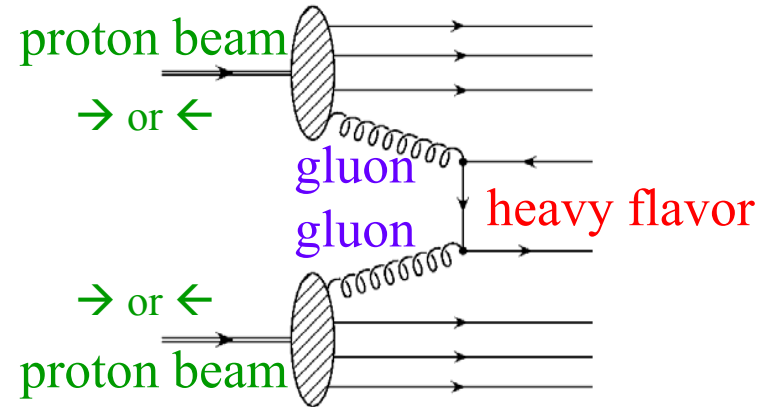
Measure particule (here  $J/\Psi$ ) yields in each configuration, that are sensible to the underlying parton distribution function

Form asymmetries:

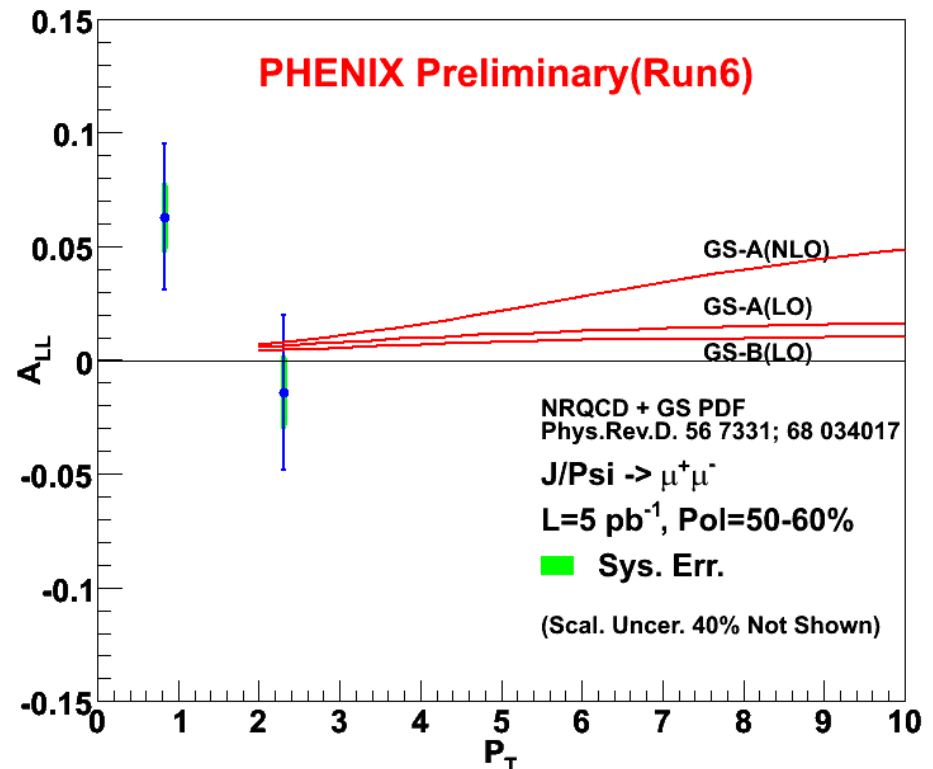
$$A_{LL}^{incl} = \frac{1}{\langle P_B \rangle \langle P_Y \rangle} \frac{N^{++} - R \cdot N^{+-}}{N^{++} + R \cdot N^{+-}}$$

$$A_{LL}^{J/\Psi} = \frac{A_{LL}^{incl} - f_{BG} \cdot A_{LL}^{BG}}{1 - f_{BG}}$$

$$\approx \frac{\Delta g(x_1)}{g(x_1)} \frac{\Delta g(x_2)}{g(x_2)} a_{LL}^{gg \rightarrow Q\bar{Q}}$$



$J/\Psi$ :  $|y| = 1.2-2.4$



# Negative binomial distribution

$$P_n^{(k)} = \frac{\Gamma(n+k)}{\Gamma(n-1)\Gamma(k)} \left( \frac{\mu/k}{1+\mu/k} \right)^n \frac{1}{(1+\mu/k)^k}$$